HOT DEFORMATION BEHAVIOUR OF Mg-Zn -Gd-Nd ALLOY

A DISSERTATION

Submitted in partial fulfilment of the

requirement for the award of the degree

Of

MASTER OF TECHNOLOGY

IN

MATERIALS ENGINEERING

Submitted by

MOHIT G. MADAVI

(16545011)

Under the supervision of

Dr. K. S. Suresh

Department of Metallurgical and Materials Engineering

Indian Institute of Technology Roorkee, Roorkee – 247667, India

May, 2018

CANDIDATE'S DECLARATION

I, here by certify that the work which had been presented in this dissertation entitled **"DEFORMATION BEHAVIOUR OF Mg-Gd-Nd-Zn ALLOY"** in the partial fulfilment of requirement for the award of the degree of Master Of Technology in the MATRIALS ENGINEERING, submitted in the department of Department of Metallurgical and Materials Engineering Indian Institute of Technology Roorkee, is genuine record of my own work carried out from July 2017 to May 2018 under the supervision of **Dr. K.S. Suresh**, assistant professor at Metallurgical and Materials Engineering Department of Indian Institute of Technology Roorkee.

Date: (MOHIT G. MADAVI)

Place: Materials Engineering.

CERTIFICATE

This is to certify that the above statement made by the candidates is correct to the best of knowledge and belief.

(Dr. K. S. Suresh)
Assistant professor,
Department of Metallurgical and Materials Engineering,
Indian Institute of Technology Roorkee, Roorkee 247667, India.

ACKNOWLEDGMENT

I would like to express my deep sense of gratitude and sincerely thankful to **Dr. K. S. Suresh**, Assistant Professor, Department of Metallurgical and Materials Engineering Indian Institute of Technology Roorkee, for his valuable guidance, continuous encouragement, valuable suggestion, the seminar that he had held for me for the betterment of my knowledge and continuous support throughout my entire course of study. The success in the dissertation work is the reflection of his innovative ideas, new concepts and hard work. I am very fortunate to work under his supervision.

I am very thankful to all faculty members & the PhD scholar for their continuous help and valuable suggestion throughout the year. I am also thank full to my friend Devang Gandhi for his continues help during my entire course of study. I also express my gratitude to lab attender Rajendra sharma, Naresh sharma and R.K. sharma for their helping nature throughout the year of my course work.

I find myself fortunate to express my love to my **family** and my **friends** for their continuous support in up & down condition of my life and giving me strength for the betterment of tomorrow.

MOHIT G. MADAVI

Materials Engineering

(16545011)

CONTENT

LIST OF FIGURES

Page No.

LIST OF TABLES

ABSTRACT

Today world needs light and high strength material as a structural material for better efficiency and high fuel efficiency application. Magnesium based alloy are an emerging light material for the same. Magnesium has attracted in the automobile industry and aerospace industry. Magnesium has improved the performance and fuel efficiency of the vehicle and aeroplanes. Light weight along with the strength has generated interest in it. However, the poor ductility and formability at low temperature, particularly at room temperature has limited the application of magnesium. People are using as cast structure until now but the use of wrought magnesium is very less due to the limited formability.

This limited formability is due to limited slip system and strong unfavourable texture formation during deformation. In order to weaken this texture small rare earth element addition has been done. Due to rare earth addition room temperature formability can be optimised.

In the present study hot deformation of the Mg-Gd-Nd-Zn alloy has been carried out and the alloy has been experimentally examined and study the effect of rare earth addition on mechanical property and its texture. The as cast Mg alloy with composition (Nd+Gd mixture 0.8-1.7 wt %), zinc (3.5-5 wt %), zirconium (0.4-1 wt %), and traces amount Mn, Fe, Cu, Ni, Si had given homogenisation heat treatment. The homogenised alloy was forged multiaxially and then compression tests of forged sample were performed. XRD analysis were done to identify the phase that are present in the alloy. Microstructure were examined using optical microscope and the Scanning Electron Microscope. Texture measurement were done using XRD and the inverse pole figure were plotted. Effect on mechanical properties were evaluated by plotting compression stress-strain curve and by analysing it. Effect on strain hardening parameter were studied by plotting hardening parameter vs. temperature inverse graph.

CHAPTER 1.

INRODUCTION

Magnesium is the lightest material among all metals having hexagonal closed pack (HCP) crystal structure along with high specific strength. The density of the magnesium is 1.74g/cm^3 which is lower value than the density of steel having density 7.86g/cm^3 and aluminium having density around 2.7g/cm^3.It can be majorly found in the earth curst. It is sixth most abundant element that can be found in the earth crust. It is largely found in minerals such as Magnesite and Dolomite. In general 850,000 tonnes of Magnesium is produced per year from the Sea containing trillions of tonnes of magnesium. The pure magnesium have melting point of 650°C and boiling point around 1091°C. Among all alkaline earth metal magnesium has lowest melting and boiling point.

Because of properties of the magnesium that is "light weight and high specific strength" has many application in different-different industry such as aircraft industry, automotive industry, electronic industry, electronic industry, and moreover it can also be used in medical sector that is in biomedical implant.

In automotive industry most of the time Magnesium metal can be used in the form of as cast structure or else in the form wrought material. For the first time people have started usage of magnesium in automotive industry in 1920. Race cars started use of magnesium for the purpose of better performance because of light weight and high specific strength. After few years later some company started use of magnesium in some commercial vehicle for the first time, for example Volkswagen. Magnesium usage has cover all the concerns of the automotive industry such fuel efficiency, increased performance and sustainability. The usage of magnesium in automotive body is in gear box, seat frames , fuel tank , car bonnets, steering columns, drivers air bag housing and in steering wheel, etc. Now a days in aerospace industry magnesium alloy named as Magnesium Elektron are used. It has improved the fuel efficiency of the aircraft and also has improved the mechanical properties and corrosion resistance of the material that could be used in manufacturing the aeroplanes.

Despite all above properties of magnesium it has one drawback that it has very low room temperature deformability as compare to structural materials such aluminium and steel. .Commercial magnesium alloys generally develop a strong basal texture during deformation by hot extrusion, which results in poor formability and ductility at room temperature [1]. Due to this it results in inadequate texture formation and microstructure formation. The texture

which develops is a strong texture which is associates with strong mechanical anisotropy. Due to above reason magnesium get fractured due to low/room temperature deformation. Hence it is very necessary to deform the material to get into desire shapes. Owing to this, addition of rare earth elements and some other alloying elements such as zirconium, zinc etc., will helps in reducing mechanical anisotropy in the material and generating weak texture during deformation. Addition of rare earth elements along with other alloying elements in magnesium will produce small grains on dynamic recrystallization (DRX) during hot deformation. Moreover traces amount of rare-earth element addition in magnesium alloys suggested to modify the crystallographic texture during extrusion, leading to the formation of a <11 -21> component parallel to the extrusion direction(ED), which is commonly referred to as RE texture [2–7]. Due to this it gives high strength. Following stress-strain curve for compression as well as for tension has and EBSD analysis will show how on rare earth addition to the magnesium has improved the strength of the material and has refine the grain size.

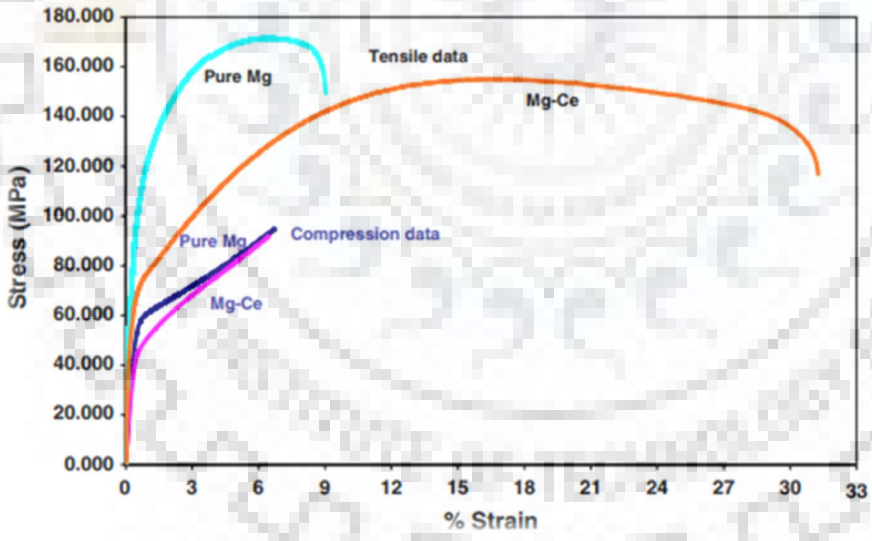

Fig 1. Tensile and compression data for extruded Mg and Mg– 0.2Ce rods (extrusion ratio =25:1). [8]

It shows that on adding cerium (rare earth element) in pure magnesium improves it's ductility in tension as well as in compression. Following is the image which shows the fully recrystallized grains than compare to pure Mg.

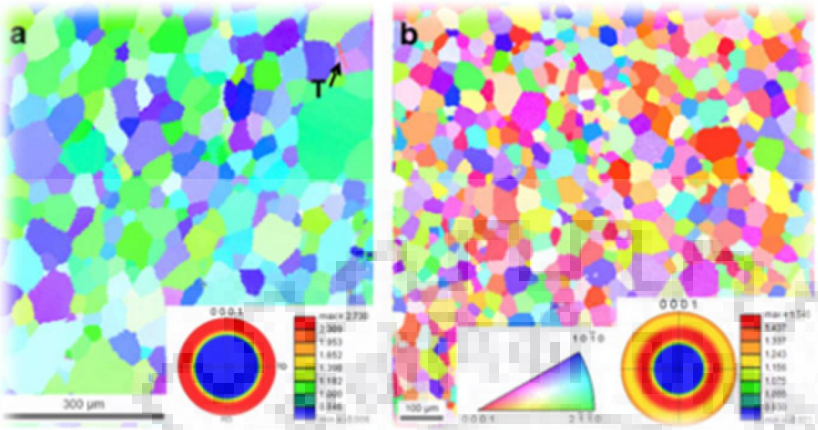

Fig 2. EBSD analysis and axial texture plots of fully recrystallized Mg (a) and Mg–0.2%Ce (b) following an extrusion ratio of 25:1. Extrusion axis is normal to image plane.[8]

CHAPTER 2

LITERATURE REVIEW

2.1 EFFECT OF RE ADDITION ON TEXTURE

D. Griffiths (2005) [9] had said in his paper that magnesium in the form of wrought product had never been/rarely had been used before due the strong texture formation during processing which results in fracture of the material when strained in particular direction but in other direction we may find ductility(anisotropic property in the material). In order to minimise the effect of strong texture formation (increasing the homogenous deformation of the material) and improve the formability of the magnesium he suggested to add rare earth elements such as yttrium, neodymium, gadolinium, cerium, lanthanum, etc. D. Griffiths also had added that minimisation of strong intensity during processing of the material is due the recrystallization that occurs during hot deformation and addition small amount of rare earth alloying elements(around 0.01% of the whole magnesium matrix).

D. Griffiths had said that the anisotropy in the magnesium material is due to the less number of slip system in the material to accommodates the deformation in the material. Magnesium is hexagonally closed packed material having three slip system along with two twinning system which get easily activated. The slip system and twinning system are listed below.

Table 1. Activated HCP slip and twining systems in magnesium.

Deformation mode	System
Basal <*a*> slip	{0001} <11-20>
Prismatic<*a*> slip	{10-10} <11-20>
Pyramidal <a> slip	{01-11} <2-1-10>
Pyramidal <a+c> slip1	{01-11} <11-2-3>
Pyramidal <a+c> slip 2	{11-22} <11-2-3>
Tension twining	{10-12} <10-11>
Compression twining	{10-11} <10-12>

D. Griffith stated that the basal slip has very low critical resolved shear stress value compared to the prismatic and pyramidal slip which leads to the formation basal texture in the material

during the time processing. Magnesium with anisotropic property gives very different-different values of yield stress and ductility when deformed in different-different direction as shown in the below diagram.

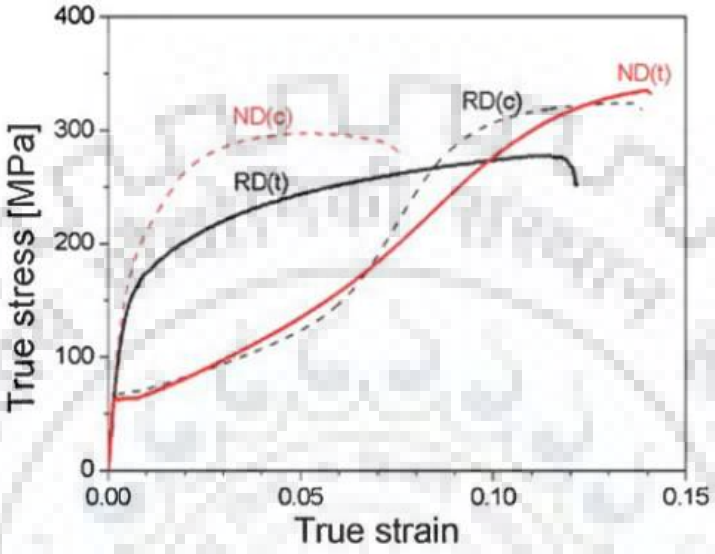

Fig 3. Variation in the stress value on loading in the different direction

D. Griffiths also stated that the increasing amount of addition of rare earth elements in the magnesium increases its ductility significantly as shown in below diagram.

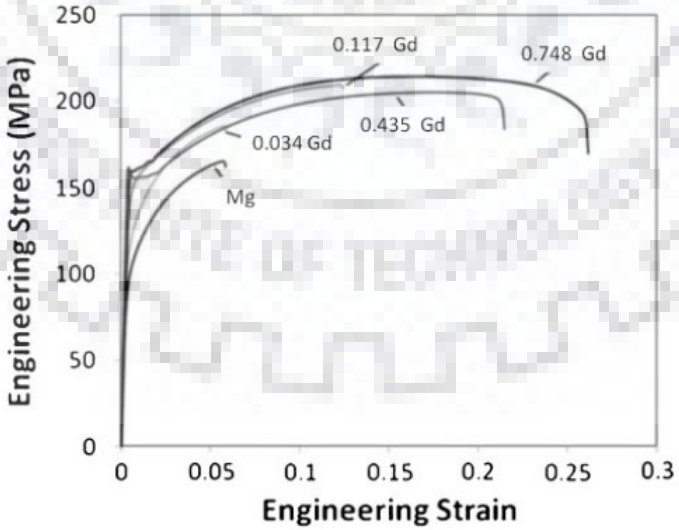

Fig 4. Variation in ductility of magnesium on alloying with increasing amount of rare earth alloy.

D. Griffiths has shown the changing texture of a rolled magnesium-gadolinium binary alloy with changing concentration of a gadolinium as follows.

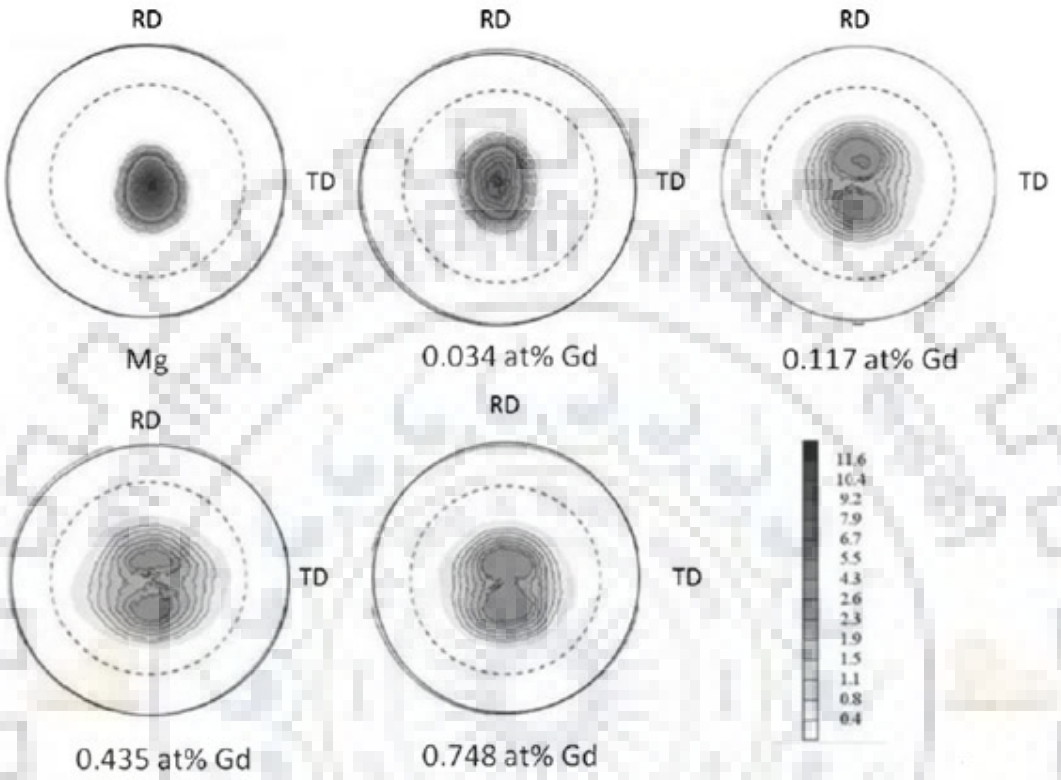

Fig 5. Varying rolled texture on changing the concentration of the rare earth element (gadolinium).

One can see that on increasing the concentration of gadolinium in the magnesium has change the intensity of the texture from 11.6 to 2.6 and has spread the texture towards the transvers direction. RE effect is changing intensity and the spreading of the texture towards the transvers direction.

Jan Bohlen [2006] [10] had analysed six alloy. Alloys and their composition are listed below in the table number 2. Alloys ZK10, ZE10, ZEK100, ZEK410, ZW41 were industrial processed and were examined in as rolled condition. Alloy ZM21 were casted and machined into the slab of dimension 240 mm×70 mm ×7.4 mm for rolling purpose.

Table 2. Properties and composition of the alloy studied.

Alloy	Avg. grain size(μm)	Zn (wt %)	Mn (wt %)	Ce (wt %)	Nd (wt %)	La (wt %)	Y (wt %)	Zr (wt. %)
ZM21	14	2.1	0.9	-	-	-	-	-
ZK10	9	1.0	-	-	-	-	-	0.3
ZE10	18	1.3	-	0.1	-	-	-	
ZEK100	9	1.3	-	0.2	-	0.1	-	0.5
ZEK410	10	4.3	-	0.7	0.2	0.2	-	0.5
ZW41	15	4.0	-	-	-	-	0.7	-

Sample were given homogenisation heat treatment for 16hr at 400°C. He had performed tensile testing on the rolled alloy on universal tensile testing machine at room temperature and at strain rate of 10^{-3} or 5×10^{-3}. After performing the tensile test samples were taken form rolled direction, 45°C and transverse direction in order to examine the texture and the microstructure.

In the analysed microstructure were found that the grain size of the ZM21 and the ZE21 were same in size around 18-22 μm. for other alloy grain size are listed in table number 2. In the microstructure precipitates were found in different amount with different composition depending upon the amount of alloying elements. EDS analysis has shown the elements which are present in the precipitates. The elements which are present in the precipitates are listed in the following table.

Table 3.Elements in precipitates in given alloy.

Alloy	Elements contain in precipitates
ZM21	Zn, Mn, Mg
ZK10	Zn, Zr, Mg
ZE10	Zn, Ce, La
ZEK100	Zn, Zr
ZEK410	Zn, Zr
ZW41	Zn, Y

Following are the microstructure of the examined alloy taken from the rolled direction.

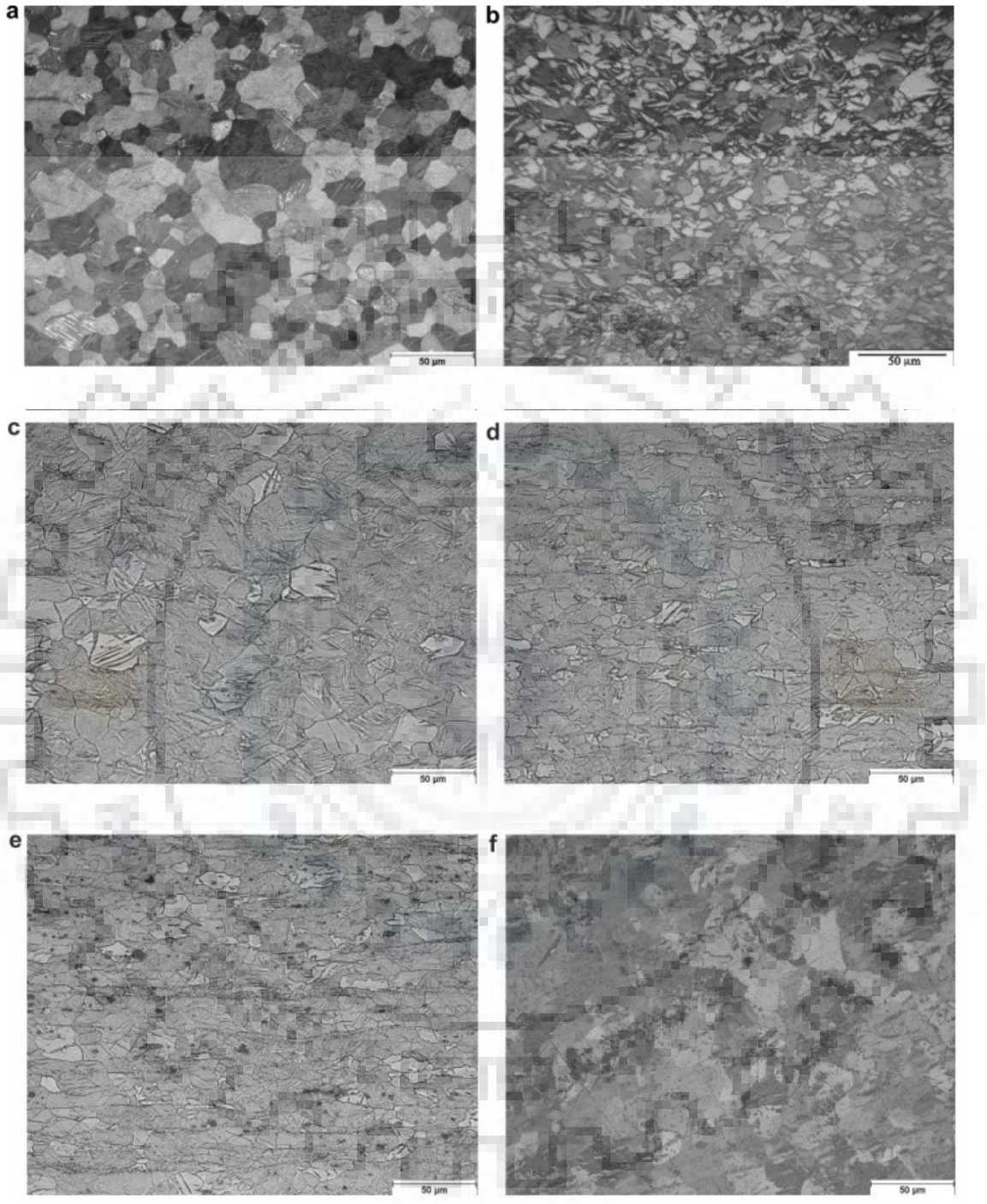

Fig. 6. Sample micrographs of magnesium sheets (RD horizontal): (a) ZM21, (b) ZK10, (c) ZE10, (d) ZEK100, (e) ZEK410 and (f) ZW41.

Grain size can be compared in given optical microstructure. Respective grain size are given in the table number 2.

Following Figure 7 shows the (00.2) and (10.0) pole figure for rolled sample.

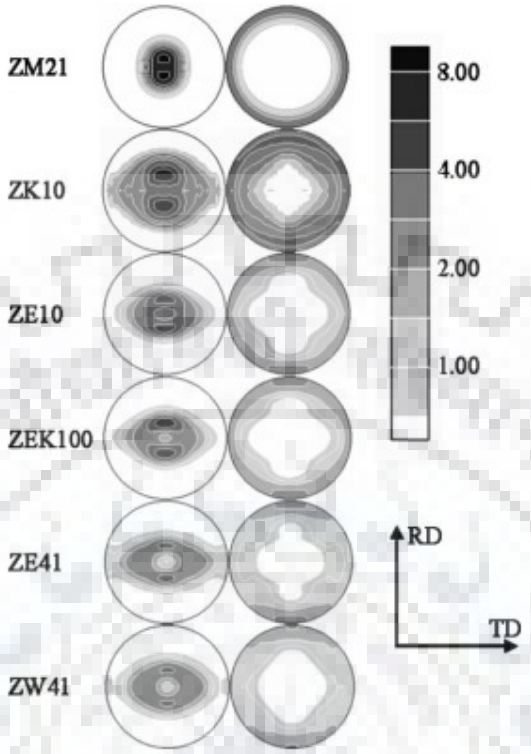

Fig 7. Equal area projection of texture measurements on rolled samples

"Basal" texture were found in the given rolled material in which majority of the grains are oriented in such way that the (00.1) basal plane are closer to the plane of rolled sheet. Variation in the strong intensity of the basal texture could be found in the pole figure above. There is variation in the exact location/orientation of the strong intensity in the given above figure. There is tilt in the peak intensity from the sheet normal direction to the rolling direction which can be seen in the figure. Weaker intensity indicate the weak texture formation. Above figure suggest that there is larger distribution of intensity in the transverse direction of the basal plane but there is no significant effect in distribution of basal plane in rolling direction. Prismatic plane (10.0) are oriented more towards the plane of the sheet that is they oriented parallel towards the rolling direction.

Following figure clearly shows the tilt in the peak intensity.

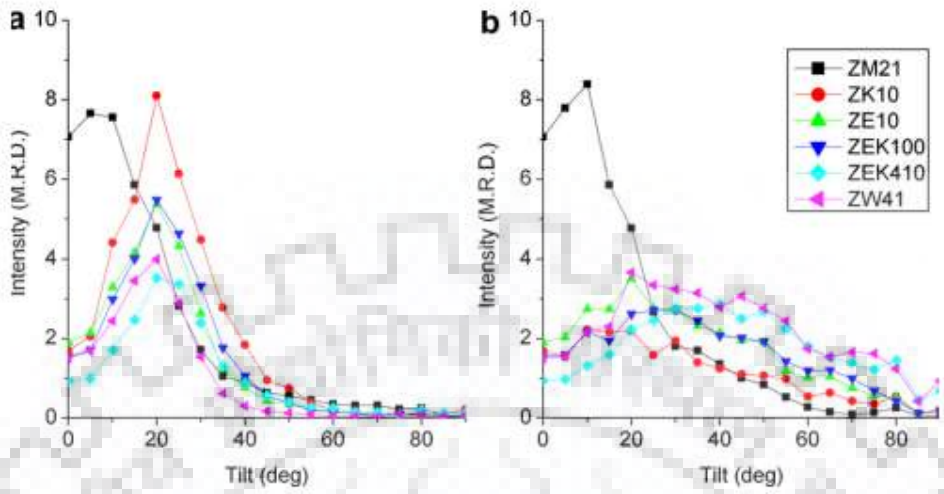

Fig 8. Texture comparison with the intensity (in multiples of a random distribution or MRD) in the basal pole figures plotted as a function of tilt from the sheet normal direction toward the (a) rolling or (b) transverse direction.

Figure 8 shows tilt in the intensity from normal direction to toward rolling and transverse direction. Above figure illustrate that the alloy ZM21 which does not contain any RE elements has shown strong basal texture. Peak texture intensity is 8 times greater than the random distribution with larger angular distribution towards rolling direction than towards the transvers direction. All other alloy containing zinc has shown lower intensity in normal direction to the sheet but has shown peak intensity in the direction +20° from normal direction to towards rolling direction. From figure one can see that the alloy ZM21 and ZK10 has shown similar peak intensity but in different direction. Jan Bohlen has observed that there is similar texture formation in between alloy ZE10 and ZEK100. Similarity in the texture formation put forward for consideration that grain refiner Zr has given no effect in texture refining. But on comparing the alloy ZK10 and other RE containing alloy in the above figure it suggest that RE addition has altered the texture in the rolling as well as in the transverse direction.

2.2 EFFECT OF CHANGE IN TEMPERATURE AND STRAIN RATE ON MICROSTRUCTURE

Li Li [11] has performed hot uniaxial compression test on the cylindrical specimen magnesium alloy (Mg–9Gd–4Y–0.6Zr) having dimension 10mm diameter and 15mm height. The hot uniaxial compression was carried in certain parameter range i.e. temperature range from 573-773 K and strain rate from 0.001/s -1/s. After compression test sectioning of the sample through compression axis were done and then microstructure were evaluated. Deformation band were easily observed in microstructure. Fig 9 shown below shows microstructure of the alloy with different deformation condition but all are strained to 0.7 (Fig 9 a only up to 0.2).

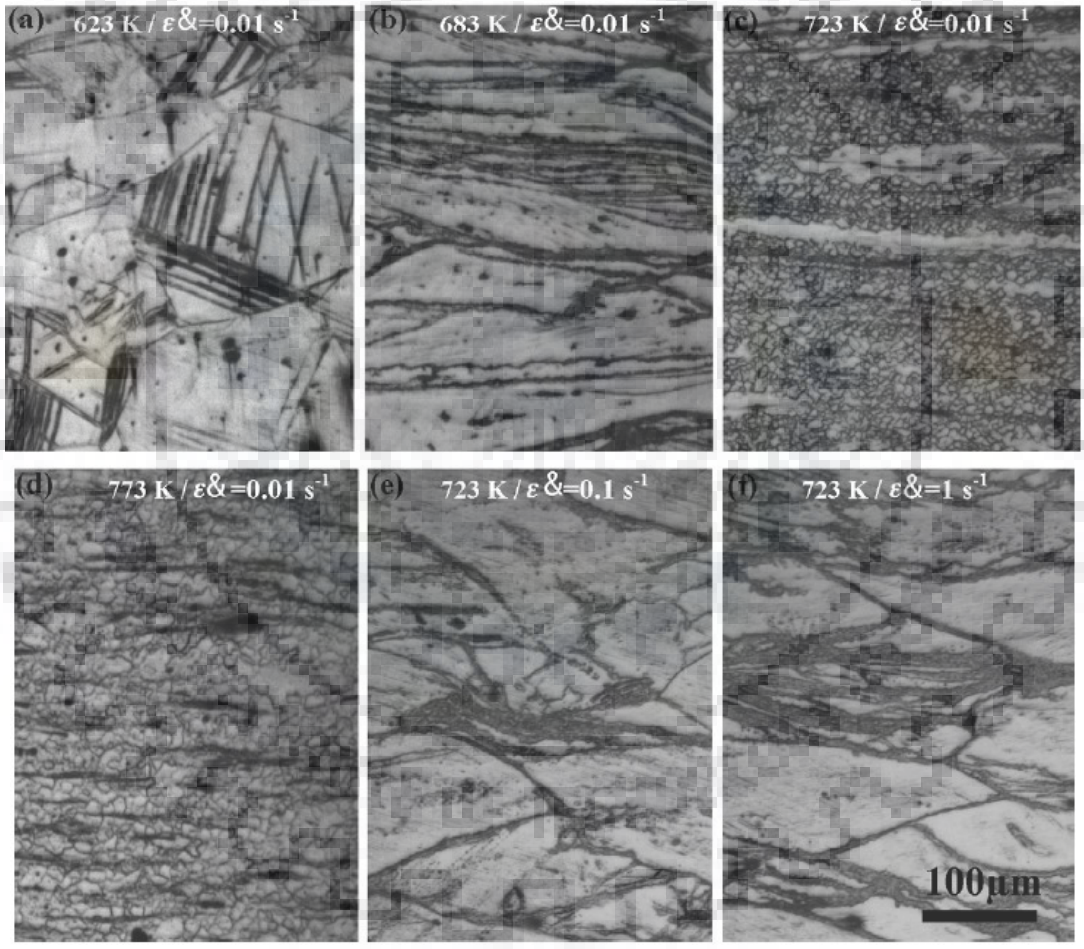

Fig 9. Optical microstructure of the alloy deformed to the strain level of 0.7 (except for (a)) at different deforming conditions, showing that post-deforming microstructure was sensitive to deformation condition. (a) 623 K, 0.01 s^{-1}; (b) 683 K, 0.01 s^{-1}; (c) 723 K, 0.01 s^{-1}; (d) 773 K, 0.01 s^{-1}; (e) 723 K, 0.1 s^{-1}; (f) 723 K, 1 s^{-1}

If we look at the Fig 9 a due limited slip system in the magnesium-Re alloy we can see twins in the microstructure which due the requirement of the high critical stress for the activation of the non-basal slip system. Due to this early mechanical fracture occur. On deforming the material in the deformation condition of temperature 683 K at strain rate of 0.01/s up to 0.7 strain shows fibrous structure in the material which is nothing but the shear band formation. It can be clearly seen from the microstructure that this shear band formation occur along the direction of the grain and sub-grain. Moreover shear bands are 90° to the direction of the uniaxial compression axis. In Fig 9(c) & Fig 9 (d) it observed that on increasing the deformation temperature dynamic recrystallization has occurred due to which the shear band formation what has been seen in the previous condition of deformation that is at temperature of 683K at strain rate of 0.01/s now completely replaced by small grain formation. In Fig 9 (e) on further increasing the parameter of deformation that is at temperature 723K and at strain rate 0.1/s necklace-type microstructure were observed in the deformation band. This type of microstructure are nothing but the small dynamic recrystallized grains in the deformation band. This indicate that the dynamic recrystallized grains formed from the deformation band. Formation of dynamic recrystallized grain is due the large dislocation slip or due to the cross slip occurred in the deformation band. In Fig 9 (f) at temperature of 723K and at strain rate of 1/s boundary of the dynamic recrystallized grains are unclear as compared to the boundary of the dynamic recrystallized grains in the Fig 9(c) and Fig 9(d). Increase in strain rate decreases the gain to grain misorientation which is the reason behind the unclear grain boundaries in the Fig 9(f).

In Fig 10, it is observed that the deformation bands are getting widen instead of formation of the dynamic recrystallized grains. Here the material is deformed at strain rate of 0.1/s ate different temperature for different strain. Figure 10 shows microstructure of the material which is deformed at above condition.

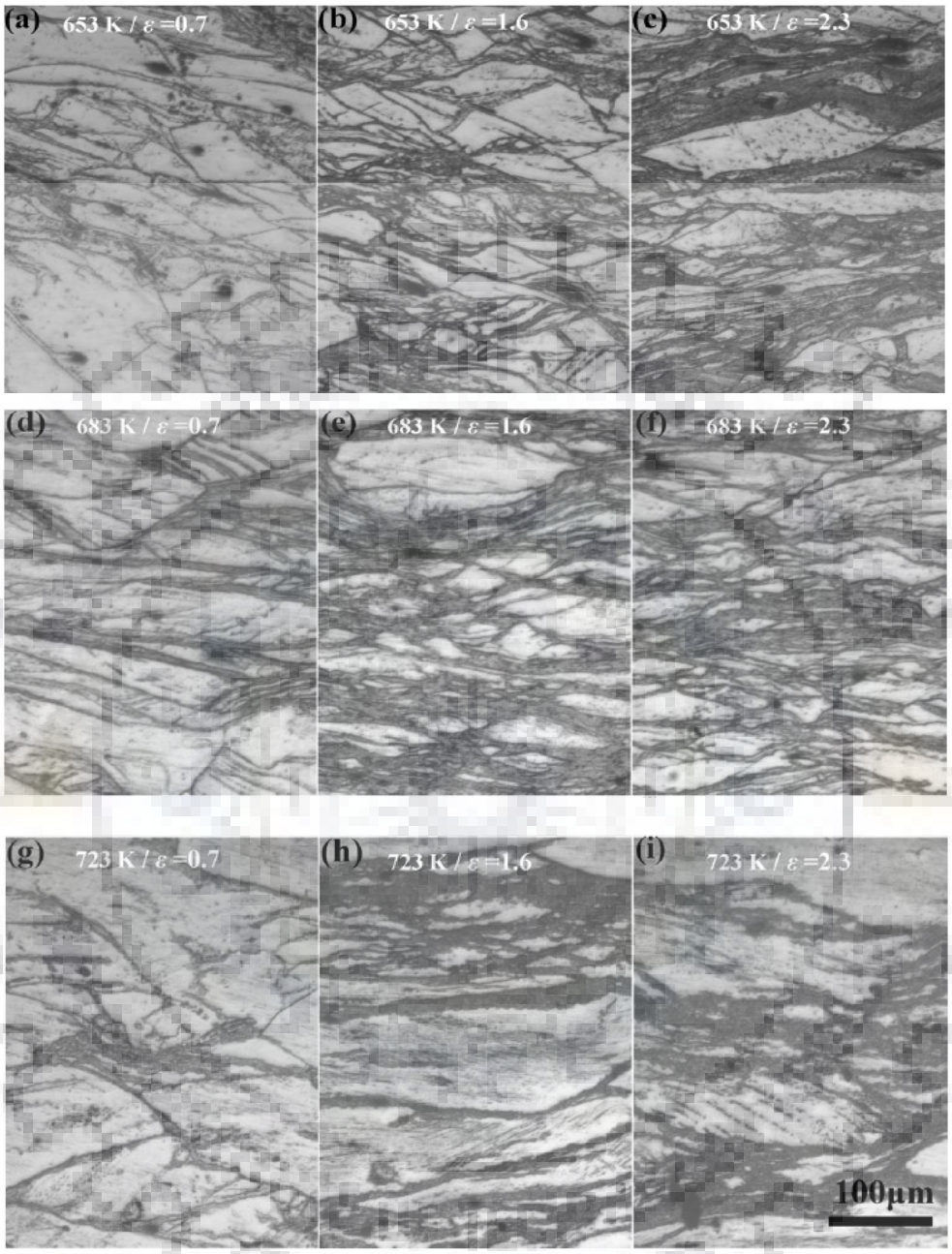

Fig 10. Microstructural evolution for the alloy subjected to hot compression at $\dot{\varepsilon}=0.1^{1}$, indicating that the deformation bands tended to widening instead of the occurrence of DRX. (a) 653 K, ε = 0.7; (b) 653 K, ε = 1.6; (c) 653 K, ε = 2.3; (d) 683 K, ε = 0.7; (e) 683 K, ε = 1.6; (f) 683 K, ε = 2.3; (g) 723 K, ε = 0.7; (h) 723 K, ε =1.6; (i) 723 K, ε = 2.3.

2.3 SOULUTE DRAG EFFECT

S.A. Farzadfar [12] has mentioned that the atomic size of the magnesium is much smaller than the atomic size of the rare earth elements for example magnesium has 173 pm atomic size whereas gadolinium has 238 pm, cerium has 242 pm, neodymium has 229 pm atomic size. In magnesium matrix due to the large size difference between the magnesium and the rare earth element, rare earth element segregate to the grain boundary or to any other defect site which minimises the atomic size misfit energy. One of the reason behind the suppression of the strong texture is due to the segregation of the rare earth elements to the grain boundary and to the defects sites.

Stanford et al. [13, 14, 15], solute and dislocation interaction is the key factor for the suppression of the strong texture. When rare earth elements segregates to the grain boundary area or to the defects sites area it does form clusters which can be very easily detected by atom probe microscopy. The clusters which are formed strongly impede the motion of the grain boundary which changes the texture of the dynamic recrystallized grain in the matrix.

Das et al. [16-18]**,** Due to the large atomic size difference rare earth elements diffuses very slowly in the matrix. Segregation of rare earth to the dislocation and the grain boundary and the slow diffusion of the rare earth elements retards the motion dislocation and the grain boundary. This impeding the motion of the dislocation and the grain boundary completely change the texture from strong texture to the weak texture i.e. nothing but the solute drag effect. Solute drag effect helps in increasing the activation energy for both the basal and non-basal plane. Solute drag is dynamic process due to which he activated basal plane can be impede by rare earth element due to which there is an increase in chances of the activation of non-basal plane. Rare earth elements oppose the dynamic recrystallization by solute drag effect (pining effect) and hence activate other slip system and twining system.

2.4 CHANGE IN MECHANICAL PROPERTY.

Jan Bohlen [2006] [10] performed tensile test on the rolled alloy on universal tensile testing machine.

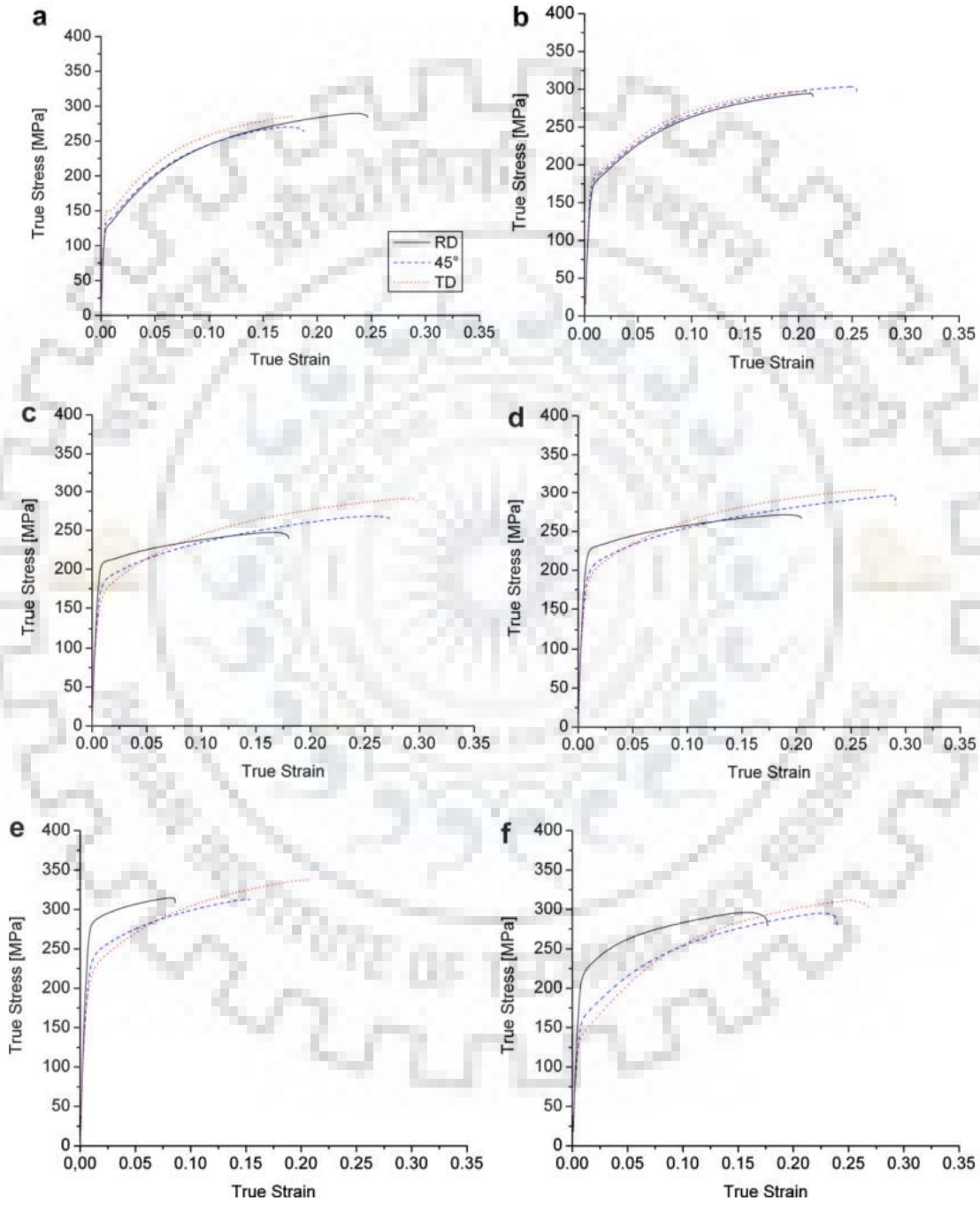

Fig 11. True stress–true strain curves from tensile tests in three sheet orientations (RD, 45, TD): (a) ZM21, (b) ZK10, (c) ZE10, (d) ZEK100, (e) ZEK410 and (f) ZWK410.

Tensile test performed at room temperature and at strain rate of 10^{-3} or 5×10^{-3}. Tensile stress-strain curve were plotted for the rolling (RD), 45° & transverse direction (TD).

Following is the table for the obtained mechanical properties.

Table 4.Results obtained from tensile test.

Alloy	Orientation	TYS(MPa)	UTS(MPa)	Elongation (%)
ZM21	RD	127	236	24.3
	45°	133	228	21.2
	TD	144	235	18.1
ZK10	RD	194	254	15.6
	45°	206	256	23.1
	TD	226	272	22.5
ZE10	RD	191	216	19.8
	45°	154	216	28.2
	TD	138	226	29.7
ZEK100	RD	203	234	23.7
	45°	163	231	39.3
	TD	154	241	31.9
ZEK410	RD	258	291	8.8
	45°	199	273	20.6
	TD	182	280	23.7
ZW41	RD	209	258	17.4
	45°	147	243	26.5
	TD	130	248	30.1

By observing the stress-strain curve and the table no 4 for alloy does not containing RE elements the yield strength is higher in the transverse direction & lower in the rolling direction and the strain to failure is larger in the rolling direction. Whereas in case of alloy containing RE elements yield strength is higher in rolling direction & lower in the transverse direction and strain to failure is lowest in the rolling direction. On observing the above results the mechanical properties for ZK10 is intermediate between the mechanical properties of ZM21 and RE containing alloy. Alloy ZEK100 shows yield strength and elongation failure greater than the

yield strength and elongation to failure of alloy ZE10. Since the ZEK alloy contains the Zr which is act as a grain refiner gives small grain in the matrix. Higher Zn contain in the ZEK410 gives higher strength but it reduces the ductility. But it is observed that ZW41 has shown low strength even the Zn containt in it is higher than the alloy ZK10 and any other alloy. Similar ductility has been seen in between ZW41 and ZEK410 alloy. It is observed that Ce and Y addition has similar effect on the texture while the mechanical properties are different.

N. Stanford (2013) [19] had performed hot compression test on the two magnesium alloy i.e. AZ31 and Mg-1.5Gd.

Table 5.Composition of the two alloys. Concentrations shown in weight per cent.

Alloy	Al	Zn	Mn	Gd	Si	Zr	Mg
AZ31	2.76	0.97	0.44	-	0.01	-	Bal.
Mg-1.5Gd	-	-	0.04	1.29	0.04	0.26	Bal.

This as cast alloys were cut into dimension of 20×15×5 mm and were deformed in plane strain compression using Glibble thermo- mechanical simulator (TMS). In TMS sample were heated until deformation temperature reached and after deformation got over sample were quenched with water. Following is the stress-strain for hot compression test.

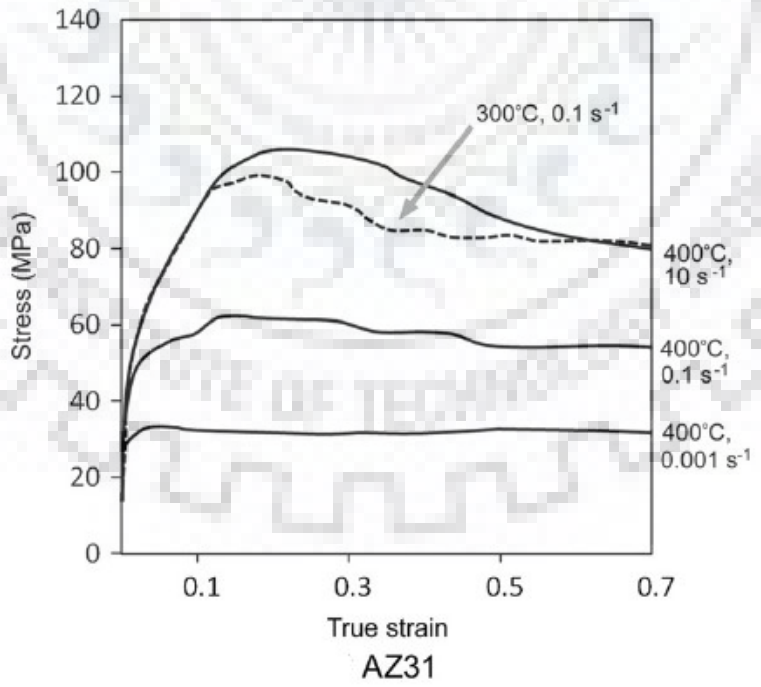

Fig 12. Flow curves obtained during plane strain compression of AZ31

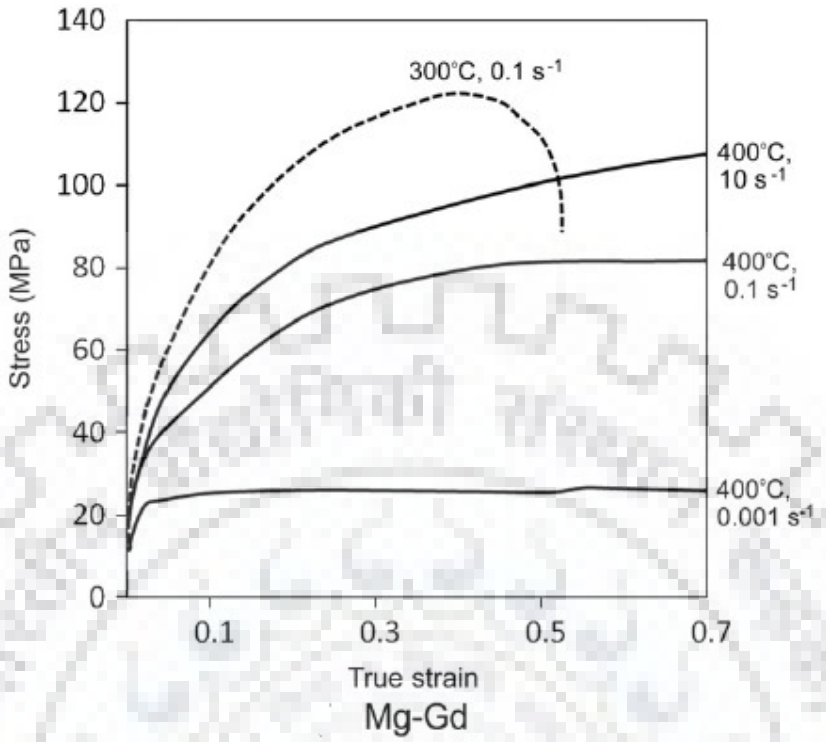

Fig 13. Flow curves obtained during plane strain compression Mg–Gd

On observing the flow curve of the alloy AZ31, there is peak in the flow curve and then softening occurs. This kind behaviour shows that the dynamic recrystallization has occurred in during compression test. But this kind of behaviour is not observed in the magnesium alloy containing rare earth elements. Sample (Mg-Gd) other than the sample deformed at 400°C and 0.001/s gives strain hardening effect as shown in the graph. On comparing the flow curve for both the alloy it is suggested that the RE addition has decrease the yield strength of the material and has improved the formability. Easy formability has been attributed as formation of weaker texture.

N. Stanford (2008) [20] has performed tensile test on five different extruded magnesium binary alloy along with one pure magnesium. Five different alloying elements were Al, Sn, Ca, La, Gd. Composition are as follows.

Table 6. Composition of alloy tested in tensile test.

Alloy	Alloy content (wt %)
Mg	-
Mg-La	0.22
Mg-Ca	0.1
Mg-Gd	1.55
Mg-Al	0.99
Mg-Sn	1.87

Before tensile testing samples were extruded in different condition. First group of sample were extruded in the condition at 450°C. 2nd group were extruded in a such way that it produces grain size around 30µm. 3rd group consist of two alloy having finer grain size 16µm.

The tensile test which carried out after extrusion is summarised in following tables and separate stress-strain curve is drawn for separate group.

Table 7. Extrusion condition and tensile test results for group 1.

Alloy	Extrusion temperature (°C)	Extruded grain size (µm)	Yield stress (MPa)	UTS (MPa)	Elongation at failure (%)
Mg	450	69	55	205	8.1
Mg-La	450	11	115	232	19.4
Mg-Ca	450	35	90	233	7.0
Mg-Gd	450	18	102	214	23.9
Mg-Al	450	40	155	248	10.7
Mg-Sn	450	58	78	239	7.5

Table 8.Extrusion conditions and grain size for specimens in Group 2

Alloy	Extrusion temperature (°C)	Extruded grain size (μm)
Mg	375	35
Mg-La	520	28
Mg-Ca	450	35
Mg-Gd	510	30
Mg-Al	440	30
Mg-Sn	450	28

Table 9. Extrusion conditions and grain size for specimens in Group 3

Alloy	Extrusion temperature (°C)	Extruded grain size (μm)
Mg	275	15
Mg-Gd	450	18

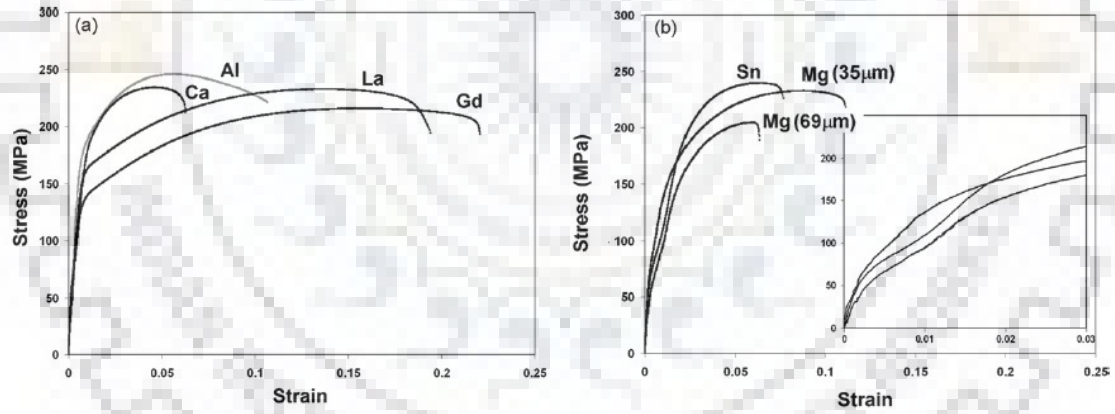

Fig 14. (a, b) Stress–strain curves for Group 1 specimens that represent alloys extruded under identical conditions. One additional pure Mg extrusion is given in (b) for comparison.

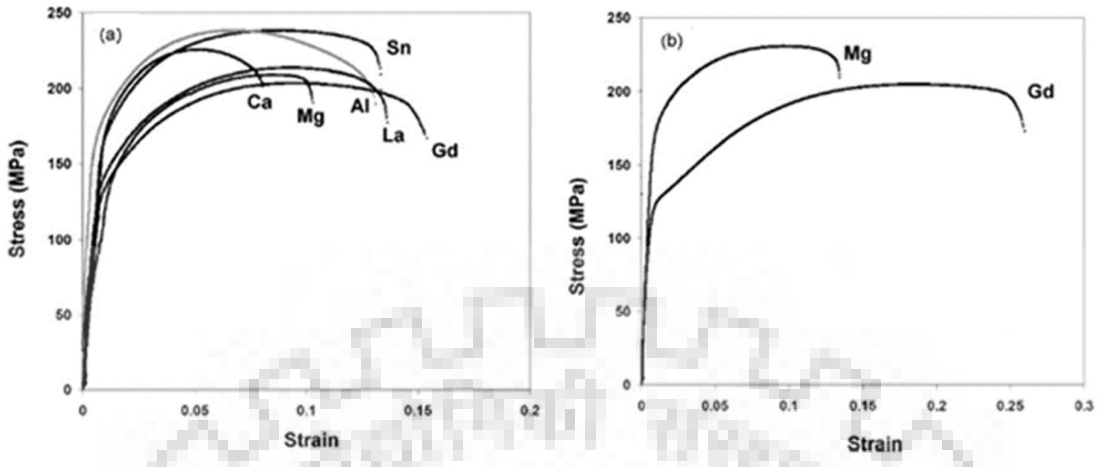

Fig 15. (a) Stress–strain curves for Group 2 specimens that all have a grain size of 30µm. (b) Stress strain curves for Group 3 comprising alloys Mg and Mg–Gd with grain sizes of 17µm.

For 1st group have variation in the grain size and has shown variation in the ductility for the sample when tensile tested as observed in the stress- strain curve. In fig b micro yielding could observe for the alloy Mg-Sn and the pure magnesium having large grain size. This behaviour is due to the large grain size formation in processing (extrusion). But this behaviour does appear in the pure magnesium having small grain size as shown in the figure.

Tensile testing was carried out for the group 2 in order to compare the ductility of the alloy having same grain size around 30µm. Table no "8" has shown the testing condition for the group 2 alloys. Five tensile testing was carried out for the one alloy for their testing condition in order to check repeatability of the properties that is getting after tensile testing. Figure below shows how the values of % elongation and tensile strength has shown deviation from one another.

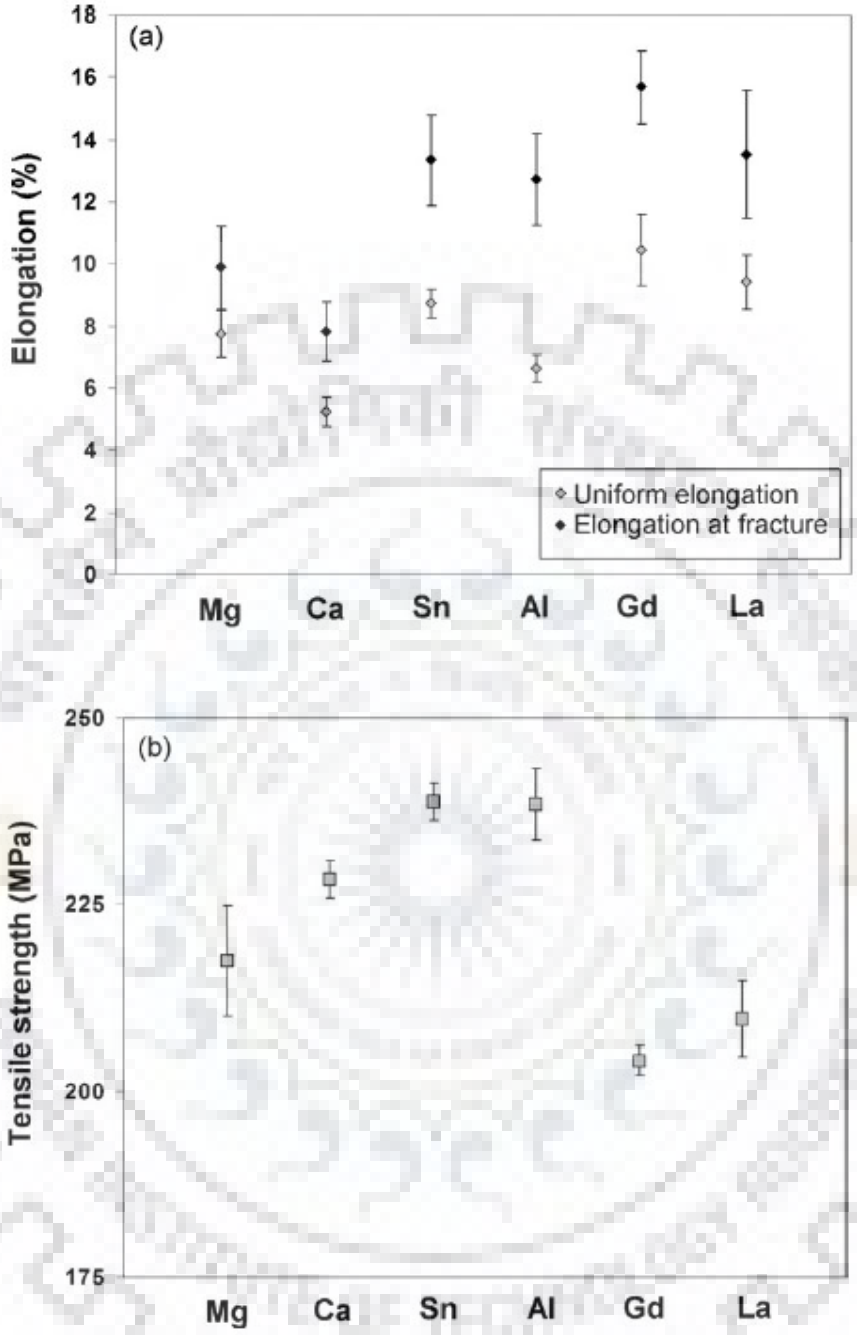

Fig 16. (a) Uniform elongation, elongation at fracture and (b) ultimate tensile strength for the six alloys in the grain size normalised Group 2. Each data point represents at least five measurements, error bars represent one standard deviation.

As observed ductility for alloy in group 1 and group 2 it is found that the variation in the ductility for alloys in group 2 is very less. All the alloy except for the Ca alloy has shown increase in elongation to failure than compare to the pure magnesium as shown in the above

figure. Similar uniform elongation has been shown for the alloy Mg-Sn and pure Mg in group 2, but higher uniform elongation has been seen for alloy containing RE elements.

Testing condition for group 3 has been given in the table no “9”. Tensile test were conducted for the alloy Mg-Gd having grain size 18μm which has shown higher ductility and pure magnesium having finer grain size 15μm which deliberately formed in order compare ductility of material having finer grains. Stress –strain curve for the group 3 is shown in the above figure where pure magnesium and Mg-Gd alloy has shown different nature of the flow curve. Pure magnesium has shown classical flow curve having work hardening and then softening of the material as similar as previous results as shown in fig a-c. But alloy Mg-Gd has shown lower value of yield strength and shown larger elongation to failure though they having similar grain size. This behaviour shows that addition of rare earth elements in magnesium produces weaker texture which results in better formability of the material than compare to the pure magnesium.

CHAPTER 3

PLAN OF WORK

As received magnesium alloy had dimension of 21cm×22cm×9cm and containing rare earth elements (Nd+Gd mixture 0.8-1.7 wt%), zinc (3.5-5 wt%), zirconium (0.4-1wt%), and traces amount Mn, Fe, Cu, Ni, Si. Cutting of rectangular block has done out of the as cast rectangular block having dimension more or less 9.5cm×9.5cm×9cm and giving homogenising heat treatment was provided in a muffle furnace at a temperature of 350°C for 3 Hr. Multiaxial forging of homogenised heat treated block was done in a forging press. Cutting of 50 cylindrical samples of dimension 10 mm diameter and 15 mm height were cut from multiaxial forged block using lathe machine or wire electric discharge machining. Prepare cylindrical sample for hot plane strain compression test by thermo mechanical simulator on Hydrawedge or Gllible. Do micro weld to all sample before hot compression test and then perform hot compression test with four different temperature and three different strain rate. Perform compression test two times for same condition. Therefore total number of sample/ test is 24 (4 ×3 ×2). Obtain data from the compression test. Plot stress-strain curve for each of the test condition. Do analysis of the stress-strain plotted for each of the condition. Compare stress-strain curve for different strain rate at same temperature by plotting the data in one graph. Calculation of strain hardening parameter for each of the condition from the obtained data. Plotting of the strain hardening parameter versus invers of temperature and analysing the obtained graph. Cutting of every sample tested in different condition through compression axis and polishing by using emery paper from 600 grit size up to 2000 grit size. Do pole figure measurement of those polished sample by XRD. Plot inverse pole figure form obtained data from XRD and do analysis of the inverse pole figure. Do XRD analysis of the as cast structure in order to identify the phase present in it. Further repolishing of the same cut sample as used for pole figure measurement form 600 grit size up to 3000 grit size and then cloth polish by using 1μm diamond polish. Prepare setup for electro polishing of the polished sample in order to get microstructure. Get microstructure from optical microscope and scanning electron microscope (SEM). Analyse the obtained microstructure from SEM and optical microscope. Now correlate all the obtained data and comment on that.

CHAPTER 4

EXPERIMENTAL PROCEDURE

An as cast magnesium rare earth alloy ingot was taken in size of 21cm×22cm×9cm. The as received material contained rare earth elements (Nd+Gd mixture 0.8-1.7 wt %), zinc (3.5-5 wt %), zirconium (0.4-1wt %), and traces amount Mn, Fe, Cu, Ni, Si. Half portion of this sample were cut into another half of size 21cm×9.5cm×9cm using same hacksaw. Material loss during cutting operation were taken care off by using small thickness blade of hacksaw. The size of the sample which is obtained by cutting of the sample by hacksaw is 9.5 cm×9.5 cm ×9 cm. Finally the sample of size 9.5 cm×9.5 cm×9 cm was kept in the muffle furnace for homogenising heat treatment at temperature around 450°C for 3 hr. Homogenising heat treatment were given in order to homogenise the chemical composition of the as cast magnesium-RE alloy. Precaution were taken care off in case of fire since pure magnesium is highly flammable material having auto ignition temperature is about 473 °C and Mg-RE alloy has ignition temperature around 530°C -740°C based on rare earth contents. The homogenised heat treated sample is then subjected to the multiaxial forging. Multiaxial forging modifies the dendritic structure which forms during casting process, into equi-axed. Dendritic structure lowers the ductility of the material leading to form isotropic properties in the material. Figure 17 represents a schematics of multiaxial forging.

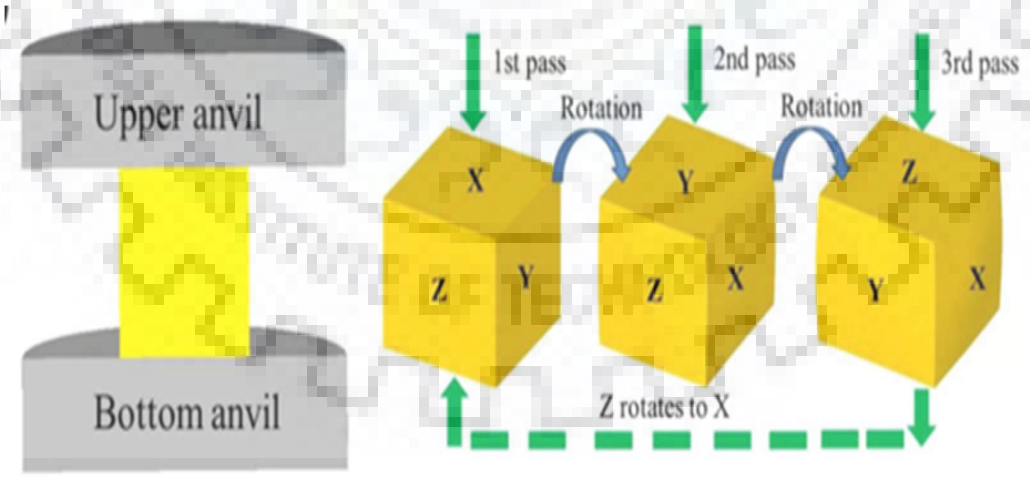

Fig 17. Multiaxial forging process.

Multiaxial forging consist of forging of the rectangular block through all of the axis i.e. through x axis, y axis & z axis. This multiaxial forging can be done by rotating the sample one by one in each direction on forging machine as shown in the Fig 17. Figure 18 shows the actual set up of forging press.

Fig 18. Actual set up of forging in laboratory

The multiaxial forged block is then cut into the 50 cylindrical sample of dimension 10 mm diameter and 15 mm in length by using wire electric discharge machining (EDM). Material loss during cutting operation were taken care off by employing the EDM machine for cutting since it gives very less material loss though price of cutting is high for wire EDM. In process of wire EDM cutting a thin single-strand metal wire, usually brass, is fed through the work piece, submerged in a tank of dielectric fluid, typically deionized water. The wire, which is constantly fed from a spool, is held between upper and lower diamond guides. The guides can move in x-y axis. The reason that the cutting width is greater than the width of the wire is

because sparking occurs from the sides of the wire to the work piece, causing erosion. WEDM gives very less material loss while cutting and can cut intricate shape also. Following figure will how WEDM cutting is done.

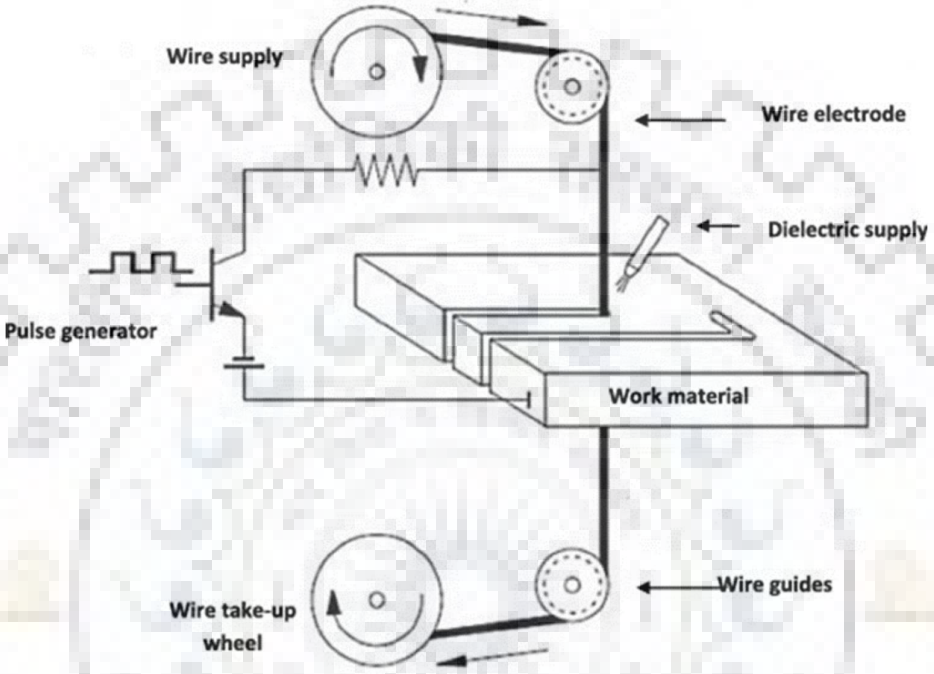

Fig 19 wire electric discharge machining.

XRD analysis were carried out of the as cast magnesium- RE alloy in order to find out the type of phases present in the magnesium-RE alloy.

Prepared cylindrical sample for hot plane strain compression test by thermo mechanical simulation on. Micro welding were done to all sample before hot compression test and then performed hot compression test with four different temperature and three different strain rate. Temperature ranging from 250°C to 400°C and strain rates were 0.1/s, 1/s, and 10/s.

Following are the set up for hot compression test and micro welding.

Fig 20. Actual set up of hot plane strain compression test.

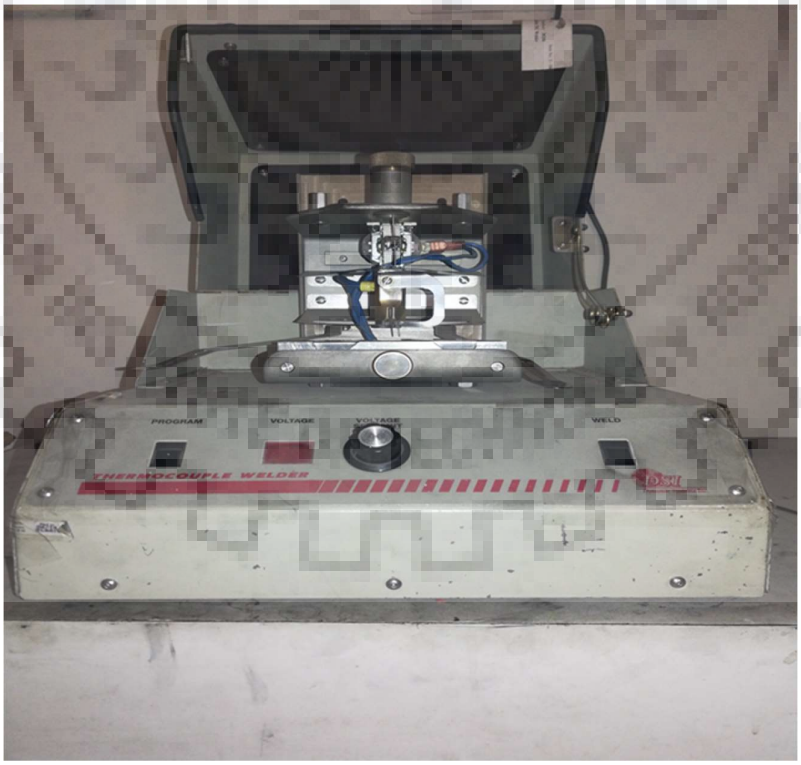

Fig 21. Actual set up of micro welding.

Following are the hot compression test condition summarised in the tabular form.

Table 10. Hot compression test parameter.

Temperature	Strain rate s^{-1}	No of samples
250°C	0.1	2
	1	2
	10	2
300°C	0.1	2
	1	2
	10	2
350°C	0.1	2
	1	2
	10	2
400°C	0.1	2
	1	2
	10	2

Hot compression tests were carried out for each of the conditions for at least two sample in order to the repeatability of the results. The data that are obtained from the hot compression tests were to correct for machine compliance. Stress-strain curve for the each and every condition were plotted using Origin 8.1 software. Stress-strain curve was plotted for the three different strain rate at same temperature in single graph and then analysed the graph. Defined strain hardening parameter here based on the literature by AT Santhanam, read hill. Graph was plotted between the calculated strain hardening parameter versus temperature inverse on the origin software. The obtained stress-strain curve and the graph between strain hardening parameter versus temperature inverse were compared for each of the testing condition.

Samples after hot compression test were cut through compression axis and polishing was done by emery paper starting from 600 mesh size up to 2000 mesh size. Inverse Pole figure measurement were done using XRD of this polished sample. The inverse pole figure were plotted .The obtained inverse pole figure were then analysed for the texture measurement.

Further repolishing of the sample were carried out using emery paper of grit size 600 to 3000 and then cloth polishing was done by using 1µm diamond paste. In order to do more precise polishing electro polishing was done. The electrolyte used for the electro polishing was 5:3 solution of ethanol and orthophosphoric acid. The time for electro polishing was 30 min keeping voltage around 1.8-1.9 volt. While performing the electro polishing liquid nitrogen were used as coolant. Electro polished sample were kept for 5-6 sec in ethanol immediately after electro polishing in order prevent sample from the oxidising. This stage is very critical stage of preventing sample from oxidising. Subsequently sample were then dried by blower and sample taken for micro imaging.

Microstructure were taken by using optical microscope (Leica) and scanning electron microscope. Images obtained from the imaging system were studied. Grain orientation and the grain size were compared with some of the sample which were tested. Finally all the results were summarised and correlate with each other in order to confirm the texture weakening.

CHAPTER 5

RESULT AND DISCUSSION

5.1 MICROSTRUCTURE

Microstructure analysis were done using optical microscope and scanning electron microscope. Figure 22 shows the microstructures of selected compression tested samples.

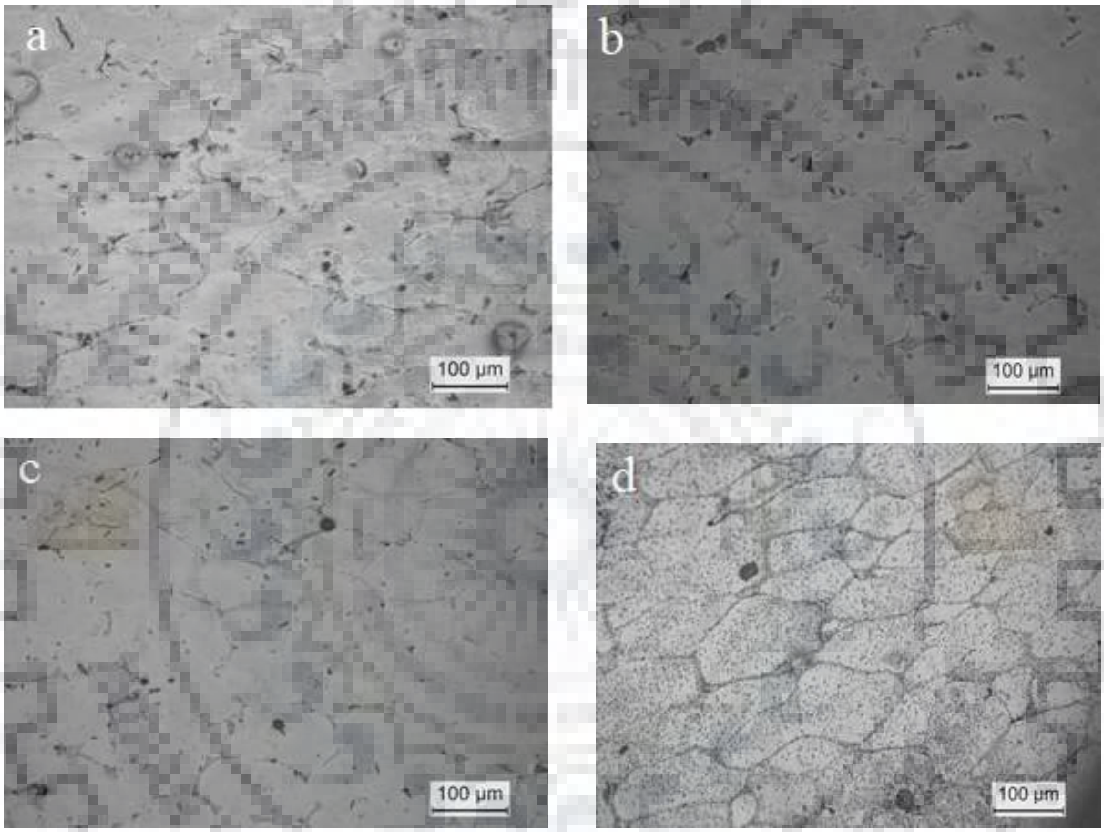

Fig 22.Optical microstructures of hot compressed sample at different temperature with 0.1^{s-1} strain rate (a)250°C; (b)300°C; (c)350°C; (d)400°C.

In the above Fig. 22 optical microstructure shows that there is elongation of grains in normal to compression direction formed at temperature of deformation at strain rate of 0.1/s. Moreover it is seen that there is precipitation of phases (RE + other alloying elements) to the grain boundary which is due to the large size difference between the magnesium and the rare earth element, rare earth element precipitates to the grain boundary or to any other defect site which minimises the atomic size misfit energy. No twins were observed from the optical or SEM micrograph.

Ii is observed from Fig 23 that comparatively there is little increment in grain size at higher temperature (400°C). If we compare the Fig 22 (d) and Fig 23 (b) it is seen that the grains are more distorted at higher strain rate.

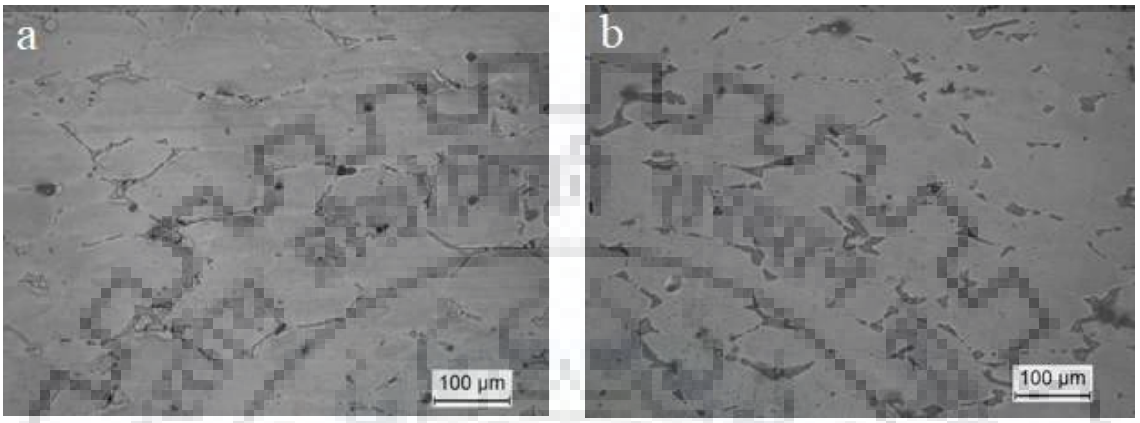

Fig 23. Optical microstructure of hot compressed sample at two different temperature with 10^{s-1} *strain rate. (a)350°C; (b) 400°C.*

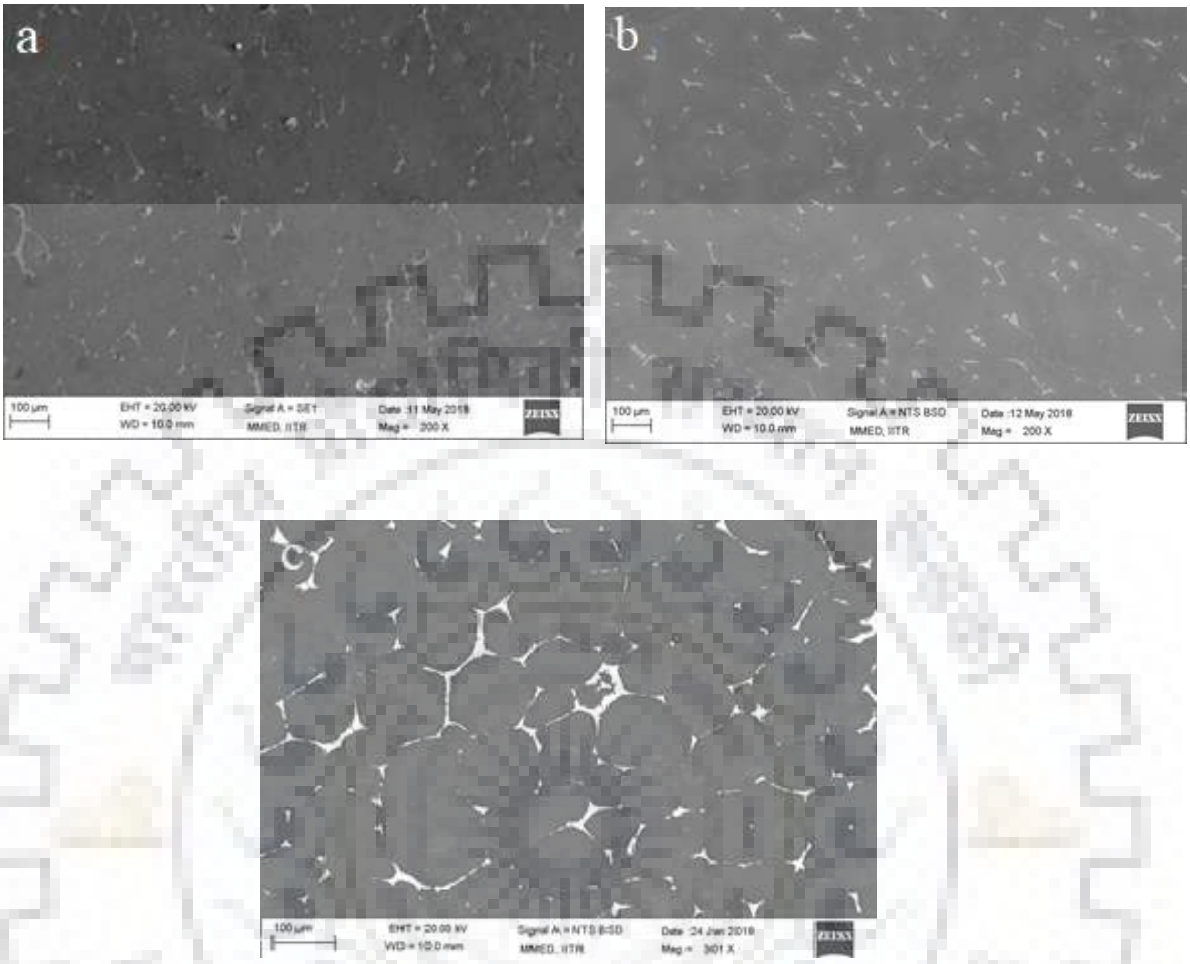

Fig 24. SEM images of hot compressed sample at three different temperature with strain rate 0.1^{s-1}. (a)250°C; (b)300°C,both at 200X; (c)400°C at 300X.

Fig 24 shows precipitation of RE element along with other alloying element in the grain boundary region. The precipitated phase was analysed by EDS in the SEM. The corresponding changes in the composition of the matrix and grain boundary phases are given in Table 11 and 12.

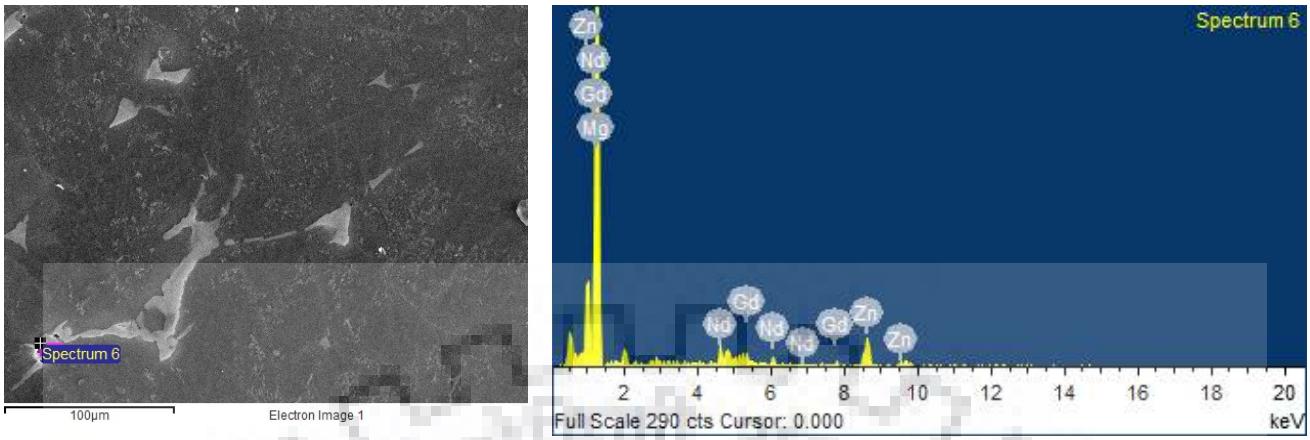

Fig 25.Phases analysis in the grain boundary region.

Table 11. Shows weight % and atomic % of elements found in phases in the grain boundary region.

Elements	Mg	Zn	Nd	Gd
Weight %	70.74	23.69	2.17	3.41
Atomic %	87.94	10.95	0.45	0.65

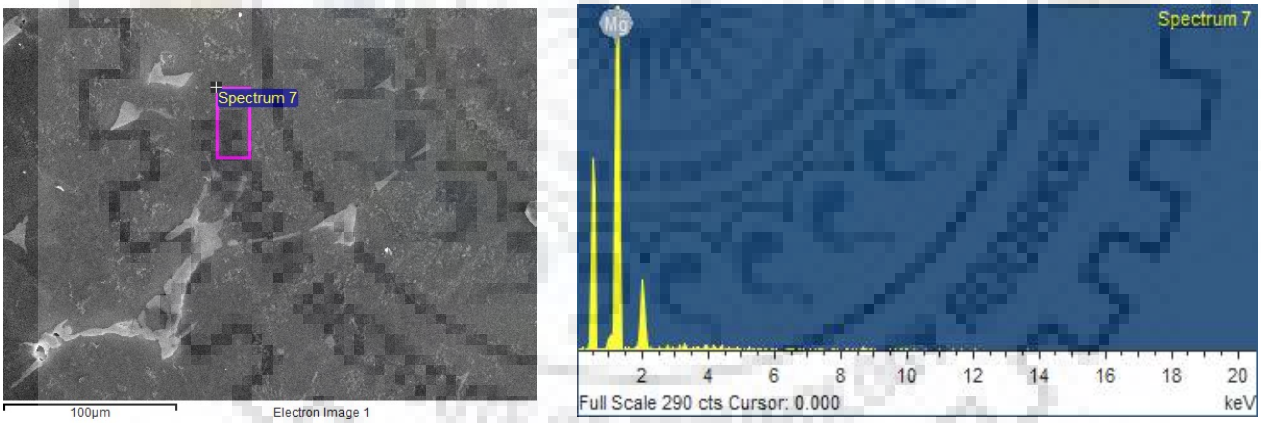

Fig 26. Phase's analysis inside the grain

Table 12. Shows weight % and atomic % of elements found in phases inside grain.

Elements	Mg
Weight %	100
Atomic %	100

5.2 XRD ANALYSIS.

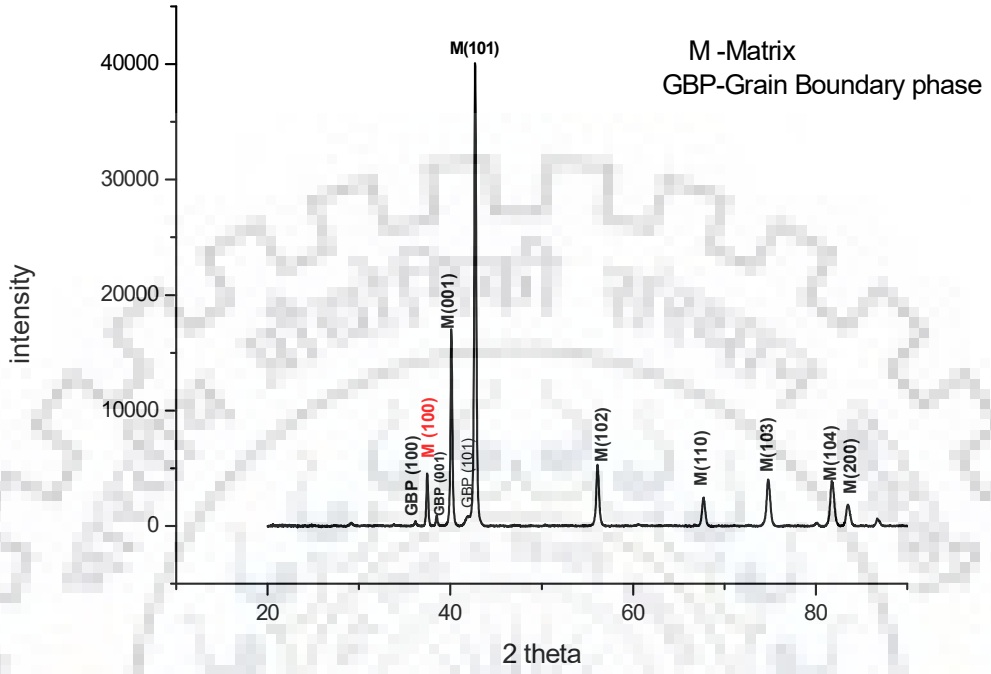

Fig 27. XRD analysis.

From the EDS analysis it is observed that the alloying additions have separately precipitated out as a grain boundary phases, while the matrix is lean of all the alloying additions.

The XRD data given in Fig 27 also contains the presence of matrix phase equivalent to magnesium and also a separate grain boundary phase having structure similar to Mg but with different lattice parameter.

5.3 TEXTURE MEASUREMENT.

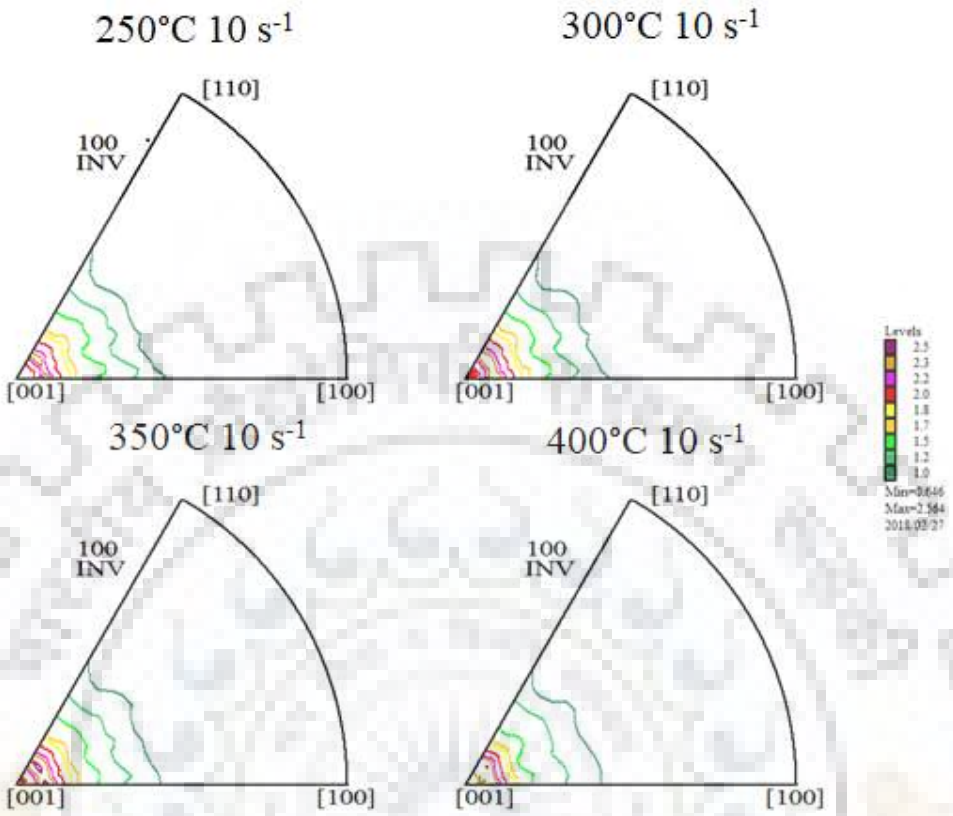

Fig 28. Inverse pole figure of compression tested sample at different temperature and 10/s strain rate along the compression axis.

From above inverse pole figure for plane (100) it can be seen that the grains are more oriented towards [001] direction i.e. it showing strong texture forming in the [001] direction and weak texture formation in the [100] &[110] direction. Inverse pole figure for the temperature 400°C and strain rate 10/s shows weak texture formation than compare to other. There is strong texture formation in [001] direction for the sample deformed at 300°C and 350°C at 10 $^{s-1}$ strain rate as compared to others.

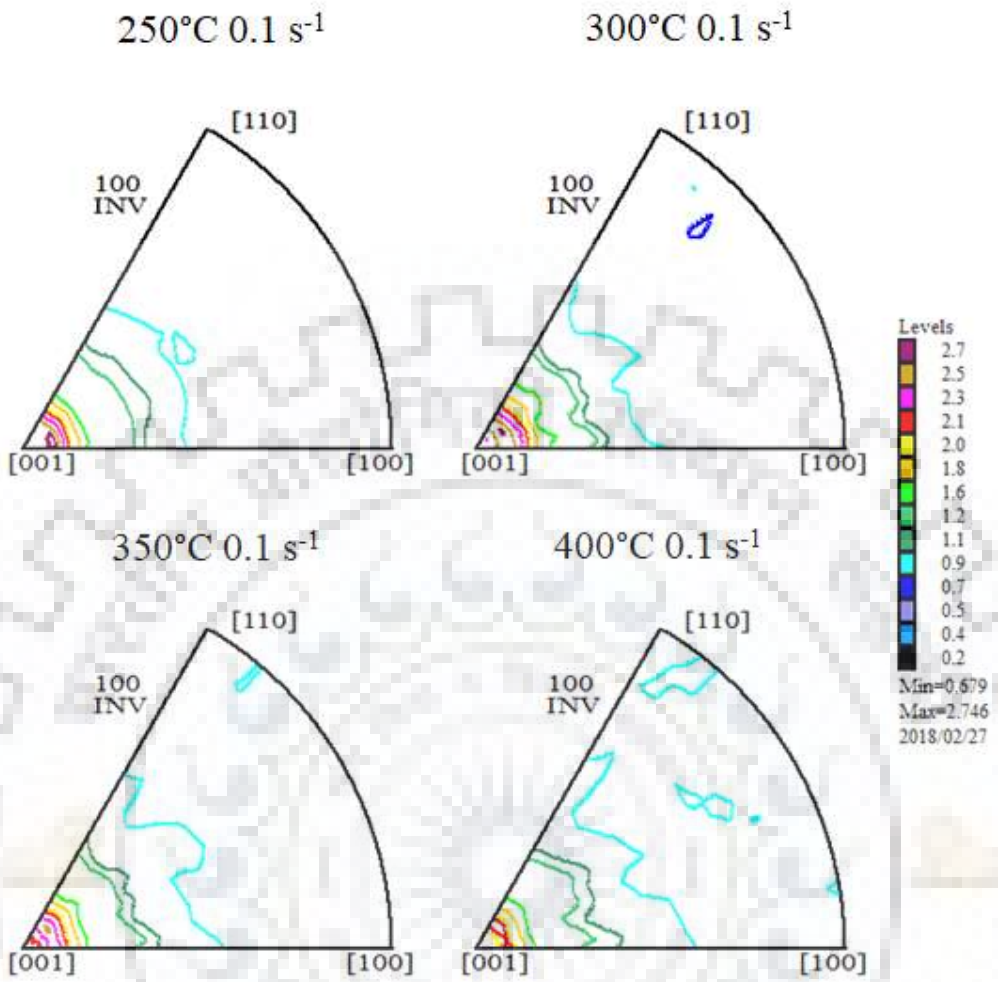

Fig 29. Inverse pole figure Inverse pole figure of compression tested sample at different temperature and 0.1/s strain rate along the compression axis.

On observing Fig 28 and 29 it is suggested that the there is a weak texture formation in the lower strain rate than compare to higher strain rate. Comparatively there is strong texture formation in the [001] direction. In Fig 29 it is observed that some of the grain with less intensity are oriented towards the [110] direction for deformation condition 400°C temperature and $0.1s^{-1}$ strain rate. The texture formation is weaker at the higher temperature.

5.4 HOT COMPRESSION TEST.

From the data of the hot compression test, stress-strain curve were plotted. Following are the stress-strain curve for the different temperature and different strain rate.

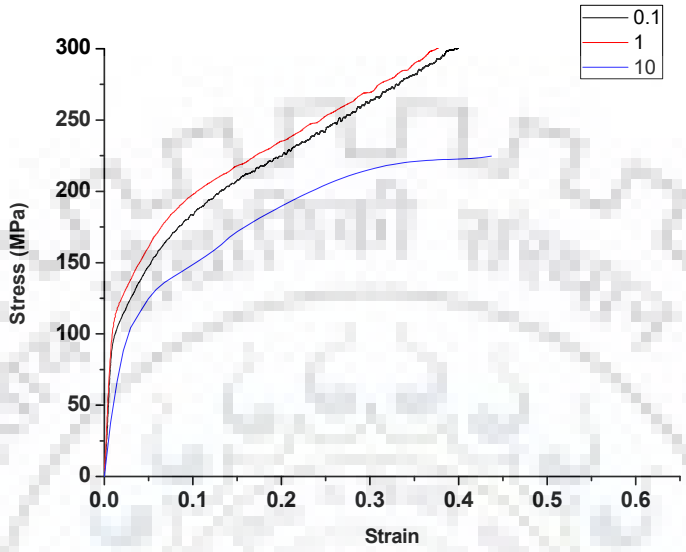

Fig 30. Stress-strain curve at 250 °C at different strain rate

The continuous increase in the stress with strain for samples deformed at 250 C could be attributed to the strain hardening behaviour. The slope of the stress-strain curve for is constant within the plastic strain range 0.3 – 0.5 for the flow curve with strain rate 0.1 s^{-1} and 1 s^{-1} Samples deformed at strain rates 0.1 and 1s^{-1} have very similar flow stress values, while a 10s^{-1} the flow stress is much lower. With increase in strain rate, an increase in flow stress value is expected. However, the decrease in flow stress value suggests that the material has negative strain rate sensitivity, at this temperature (250°C) & strain rate (10 s^{-1})

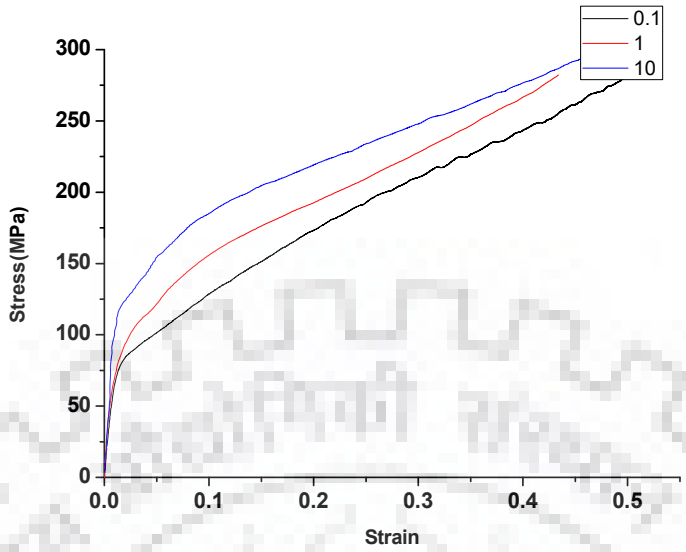

Fig 31. Stress-strain curve at 300°C at different strain rate

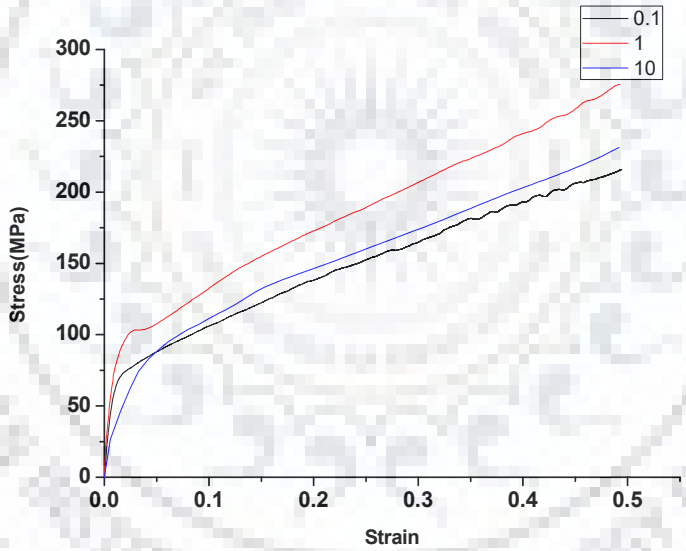

Fig 32. Stress-strain curve at 350°C at different strain rate

From the stress- strain curve is Fig 31, it can be seen that the flow stress value for the component deformed at higher strain rate showing higher flow stress value, as expected. In the flow curve of the sample deformed at the higher strain rate showing little increment and then showing decrement in the slop which shows the strain hardening and then subsequent dynamic restoration.

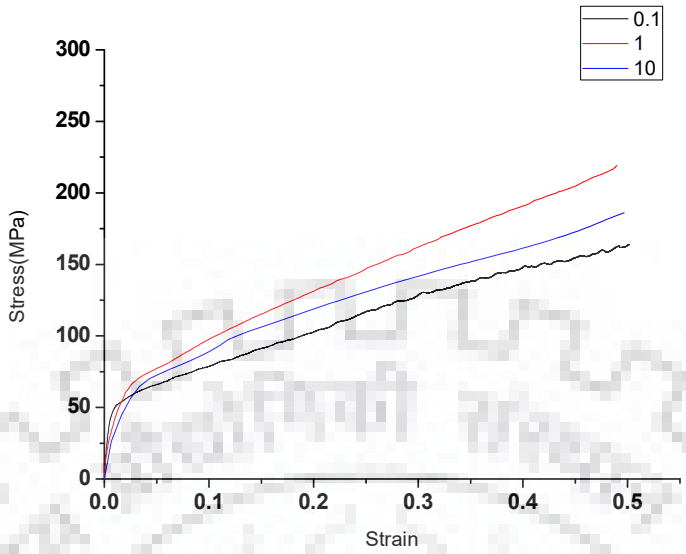

Fig 33. Stress- strain curve at 400°C at different strain rate

In the fig no 32 and fig no. 33 flow curve for both 0.1 s^{-1} strain rate and 10 s^{-1} strain rate showing almost similar behaviour, while flow curve for the 1 s^{-1} strain rate showing higher flow stress value. The flow stress value for the flow curve with strain rate 10 s^{-1} must show higher value than other flow stress value deformed at lower strain rate. Hence this behaviour shows that the material having negative strain rate sensitivity. In the Fig 32 flow curve for the 0.1/s strain rate shows that material first experiencing strain hardening behaviour and then subsequent dynamic recrystallization.

In general stress value increases on increasing the strain rate and stress value decrease on increasing the temperature. When we increase the temperature of deformation no. of slip system get activated and dynamic recrystallization occur and hence material get easily flow with low stress value during deformation.

5.5 EFFECT OF TEMPERATURE AND THE STRAIN RATE ON STRAIN HARDENING PARAMETER.

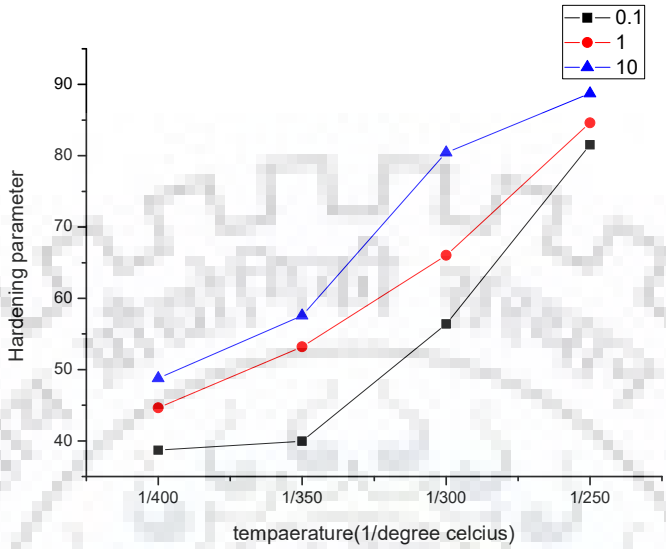

Fig 34. Hardening parameter vs. 1/T at different strain rate

In the above figure no 34, it is observed that the hardening parameter goes on increasing as we increase the strain rate and decrease the temperature. In the figure it is observed that at both lower strain rate i.e. at 0.1 s^{-1} and at 1 s^{-1}, strain hardening is steeply increasing in the lower temperature range 250°C and 300°C as expected. In case of 0.1 s^{-1} strain rate and temperature range 350°C and 400°C slope is very less as compared to other which shows that dynamic recrystallization mechanism dominates more than the strain hardening mechanism. Unexpectedly the slope for the larger strain rate shows lower value at temperature range 250°C-300°C and shoving larger value at temperature range 300°C-350°C.

CHAPTER 6

CONCLUSION

Optical microstructure shows that grains are elongated in the direction normal to compression axis at temperature of deformation at strain rate of 0.1 s^{-1}. Some phases are seen to be precipitated at the grain boundary. This phase composition has been confirmed by EDS using SEM. This phase distribution can be seen in the SEM images. Second phase which are at the grain boundary restrict the grain boundary motion hence restrict the grain growth during dynamic recrystallization which leads to formation of small grain and hence forming random orientation of the grain.

XRD analysis has confirmed the phases that could formed in the material. Texture analysis shows that there is strong texture formation with [0001] parallel to compression direction. There is strong texture formation in [001] direction for the sample deformed at 250°C and 300°C at 10 s^{-1}strain rate as compared to others. Weak texture is observed at 400°C for both the strain rates.

Hot plane stain compression data suggested that the material shows negative strain rate sensitivity at 10 s^{-1} strain rate for temperature 250°C. Increment and subsequent decrement in plastic region of the flow curve suggested that there is first strain hardening of the material then subsequent dynamic recrystallization is occurring.

It is observed that the hardening parameter goes on increasing as we increase the strain rate and decrease the temperature. Strain hardening is more dominant in the low temperature and at low strain rate as observed in the hardening parameters vs. temperature invers graph. But in the hardening parameters vs. temperature inverse graph shows low value of slope for the strain rate 10 s^{-1} at temperature range 300°C-350°C than compare to in the temperature range 250°C-300°C. This behaviour could be possible due to negative strain rate sensitivity.

CHAPTER 7

SCOPE FOR FUTURE WORK

Magnesium as lightest material and with higher specific strength among all structural material could replace all of them. In the present study texture weakening has been studied using multiaxial forging process but in future texture weakening could be study either by rolling process or by extrusion process of deformation. EBSD (electron backscattered diffraction) analysis could be done on compressed sample so that the information about distribution of grain size as well as grain orientation could get. TEM analysis could be done for precise microstructural analysis.

The study of the hot compression test at lower temperature and at higher strain rate should be done more precisely. Study on finding easier and more economical way of texture weakening should be done.

.

REFFERENCE.

[1]. M.G. Jiang , C. Xuc, T. Nakata, H. Yana,, R.S.Chen , S. Kamad , Rare earth texture and improved ductility in a Mg-Zn-Gd alloy after high-speed extrusion , Materials Science & Engineering A667 (2016) 233–239

[2] N. Stanford, M.R. Barnett, The origin of "rare earth" texture development in extruded Mg-based alloys and its effect on tensile ductility, Mater. Sci. Eng. A 496 (2008)399–408.

[3] N. Stanford, D. Atwell, A. Beer, C. Davies, M. Barnett, Effect of micro alloying with rare-earth elements on the texture of extruded magnesium-based alloys, Scr.Mater.59(2008)772–775.

[4] N. Stanford, Micro-alloying Mg with Y, Ce, Gd and La for texture modification —a comparative study, Mater. Sci. Eng. A 527 (2010) 2669–2677.

[5] J. Bohlen, S. Yi, D. Letzig, K. U. Kainer, Effect of rare earth elements on the microstructure and texture development in magnesium–manganese alloys during extrusion, Mater. Sci. Eng. A 527 (2010) 7092–7098.

[6] A. A. Luo, R. K. Mishra, A. K. Sachdev, High-ductility magnesium–zinc–cerium extrusion alloys, Scr. Mater. 64 (2011) 410–413.

[7] N. Zhou, Z. Zhang, L. Jin, J. Dong, B. Chen, W. Ding, Ductility improvement by twinning and twin–slip interaction in a Mg-Yalloy,Mater.Des.56(2014) 966–974.

[8] R. K. Mishra, A. K. Gupta, P. R. Rao, A. K. Sachdev, A. M. Kumard and A.A. Luo, Influence of cerium on the texture and ductility of magnesium extrusions, Scripta Materialia 59 (2008) 562–565.

[9] D. Griffiths (2015), Explaining texture weakening and improved formability in magnesium rare earth alloys, Materials Science and Technology, 31:1, 10-24, DOI.

[10] Jan Bohlen, Marcus R, Nurnberg, Jeremy W. Senn, Dietmar Letzig, Sean R. Agnew, The texture and anisotropy of magnesium–zinc–rare earth alloy sheets, Acta Materialia 55 (2007) 2101–2112.

[11] Li Li, Deformation band and texture of a cast Mg–RE alloy under uniaxial hot compression , Materials Science and Engineering A 528 (2011) 7178– 7185.

[12]S.A. Farzadfar, E. Martin, M. Sanjari, E. Essadiqi, S. Yue, J. Mater. Sci. 47 (2012) 5488‑5500.

[13] N. Stanford, M.R. Barnett, Mat. Sci. Eng. A 496 (2008) 399‑ 408.

[14] N. Stanford, G. Sha, J.H. Xia, S.P. Ringer, M.R. Barnett, Scr. Mater. 65 (2011) 919‑921.

[15] N. Stanford, G. Sha, A. La Fontaine, M.R. Barnett, S.P. Ringer, Metall. Mater. Trans. A 40 (2009) 2480–2487.

[16] S.K. Das, Y.-M. Kim, T.K. Ha, R. Gauvin, I.-H. Jung Metall. Mater. Trans. A, 44 (2013), pp. 2539-2547.

[17] S.K. Das, Y.-M. Kim, T.K. Ha, I.-H. Jung Calphad, 42 (2013), pp. 51-58.

[18] S.K. Das, Y.-B. Kang, T. Ha, I.-H. Jung Acta Mater. 71 (2014), pp. 164-175.

[19] N. Stanford, M. D. Callaghan, B. de Jong, The effect of rare earth elements o the behaviour of magnesium-based alloys: Part1—Hot deformation behaviour, Materials Science & Engineering A 565 (2013) 459–468.

[20] N. Stanford, M.R. Barnett, The origin of "rare earth" texture development in extruded Mg-based alloys and its effect on tensile ductility, Materials Science and Engineering A 496 (2008) 399–408.